

## Novel Benzisoxazole Derivatives as Potent and Selective Inhibitors of Acetylcholinesterase

Anabella Villalobos,<sup>\*,†</sup> James F. Blake,<sup>\*,‡</sup> C. Kelly Biggers, Todd W. Butler, Douglas S. Chapin, Yuhpyng L. Chen, Jeffrey L. Ives, Shawn B. Jones, Dane R. Liston, Arthur A. Nagel, Deane M. Nason, Jann A. Nielsen, Ismail A. Shalaby, and W. Frost White

Departments of Medicinal Chemistry, of Neuroscience and Cancer, and of Computational Chemistry, Central Research Division, Pfizer Inc., Groton, Connecticut 06340

Received April 29, 1994<sup>⊗</sup>

A series of *N*-benzylpiperidine benzisoxazoles has been developed as potent and selective inhibitors of the enzyme acetylcholinesterase (AChE). The benzisoxazole heterocycle was found to be an appropriate bioisosteric replacement for the benzoyl functionality present in the *N*-benzylpiperidine class of inhibitors. The title compounds were synthesized by alkylating 3-methyl-1,2-benzisoxazoles with an iodo piperidine derivative as the key step. Benzisoxazoles **1b-j,o** displayed potent inhibition of AChE *in vitro* with IC<sub>50</sub>'s = 0.8–14 nM. Particularly interesting were *N*-acetyl and morpholino derivatives **1g** (IC<sub>50</sub> = 3 nM) and **1j** (IC<sub>50</sub> = 0.8 nM), respectively, which displayed outstanding selectivity for acetyl- over butyrylcholinesterase, in excess of 3 orders of magnitude. *N*-Acetyl **1g** also displayed a favorable profile *in vivo*. This analog showed a dose-dependent elevation of total acetylcholine in mouse forebrain after oral administration with an ED<sub>50</sub> = 2.4 mg/kg. In addition, **1g** was able to reverse amnesia in a mouse passive avoidance model at doses of 3.2 and 5.6 mg/kg with an average reversal of 89.7%. Molecular dynamics simulations were used to study the possible binding modes of *N*-benzylpiperidine benzisoxazoles to AChE from *Torpedo californica*. Key structural insights were obtained regarding the potency of this class of inhibitors. Specifically, Asp-72, Trp-84, Trp-279, Phe-288, and Phe-330 are implicated in the binding of these inhibitors. The *N*-benzylpiperidine benzisoxazoles may be suitable compounds for the palliative treatment of Alzheimer's Disease.

The cholinergic hypothesis postulates that memory impairments in patients with Alzheimer's Disease (AD) result from a deficit of cholinergic functions in the brain.<sup>1</sup> Activity of cholinergic markers such as choline acetyltransferase is markedly reduced in the brains of patients with AD in comparison to age-matched controls.<sup>2</sup> In addition, cholinergic neurons which originate at the nucleus basalis of Meynert and project into the hippocampus and cortex show extensive degeneration in AD.<sup>3</sup> Furthermore, muscarinic antagonists such as scopolamine can induce memory impairments in normal subjects similar to that of normal aging.<sup>4</sup> As a consequence, potentiation of central cholinergic action has been proposed as an approach for the palliative treatment of mild to moderate cases of AD.<sup>5</sup>

One strategy to enhance cholinergic neurotransmission is to inhibit acetylcholinesterase (AChE),<sup>5</sup> the enzyme responsible for the metabolic breakdown of acetylcholine (ACh). Clinical studies with AChE inhibitors have produced mixed results but suggest that these agents may be able to enhance memory in patients with AD.<sup>6</sup> Treatment with 1,2,3,4-tetrahydro-9-aminoacridine (THA, Figure 1) has demonstrated moderate but significant efficacy in AD.<sup>7</sup> THA was recently approved by the FDA,<sup>8</sup> becoming the first available treatment for AD in the United States. However, the aminoacridines suffer from dose-limiting hepatotoxic effects<sup>7,9</sup> which are believed to be structure related.<sup>10</sup> Physostigmine (Figure 1), a carbamate-type inhibitor, has shown inconclusive results in the clinic possibly due to its short half-

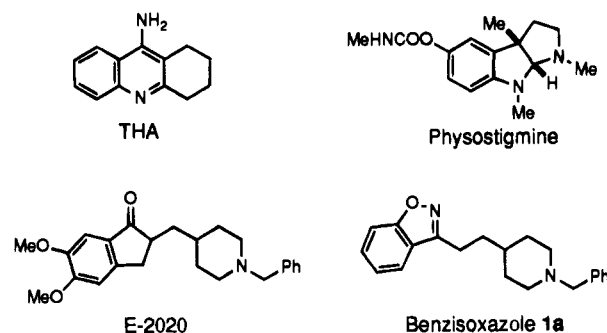


Figure 1. Acetylcholinesterase inhibitors.

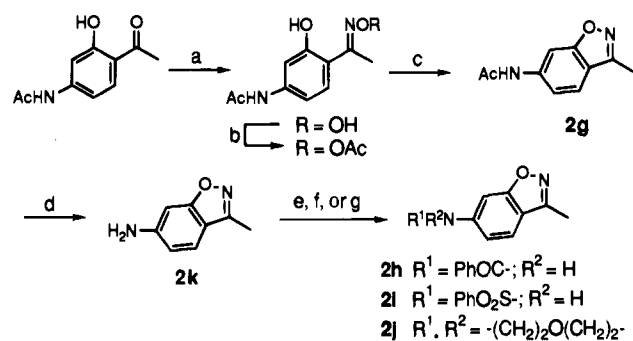
life and narrow therapeutic index.<sup>6b,11</sup> A controlled-release formulation of physostigmine is currently in phase III trials by Forest Laboratories.<sup>12</sup>

A third class of AChE inhibitors, the *N*-benzylpiperidines,<sup>13</sup> seems to overcome the unfavorable side effect profile and poor pharmacokinetics associated with the above two classes.<sup>14</sup> In addition, the *N*-benzylpiperidines display good selectivity *in vitro* for acetyl- over butyrylcholinesterase.<sup>13</sup> We became interested in exploring this class of inhibitors, represented by E-2020<sup>13c</sup> (Figure 1). The benzoyl-containing functionality and the *N*-benzylpiperidine moiety are believed to be key features for binding and inhibition of AChE.<sup>13c</sup> Our goal was to design and synthesize novel prototypes which would incorporate bioisosteric replacements for the benzoyl moiety. Furthermore, a strategy was envisioned in which the novel prototypes would be devoid of chiral centers that could undergo facile racemization. E-2020 has been tested as a mixture of enantiomers, presumably due to the ease of racemization of the chiral  $\alpha$ -keto

<sup>†</sup> Department of Medicinal Chemistry.

<sup>‡</sup> Department of Computational Chemistry.

<sup>⊗</sup> Abstract published in *Advance ACS Abstracts*, July 15, 1994.

Scheme 1<sup>a</sup>

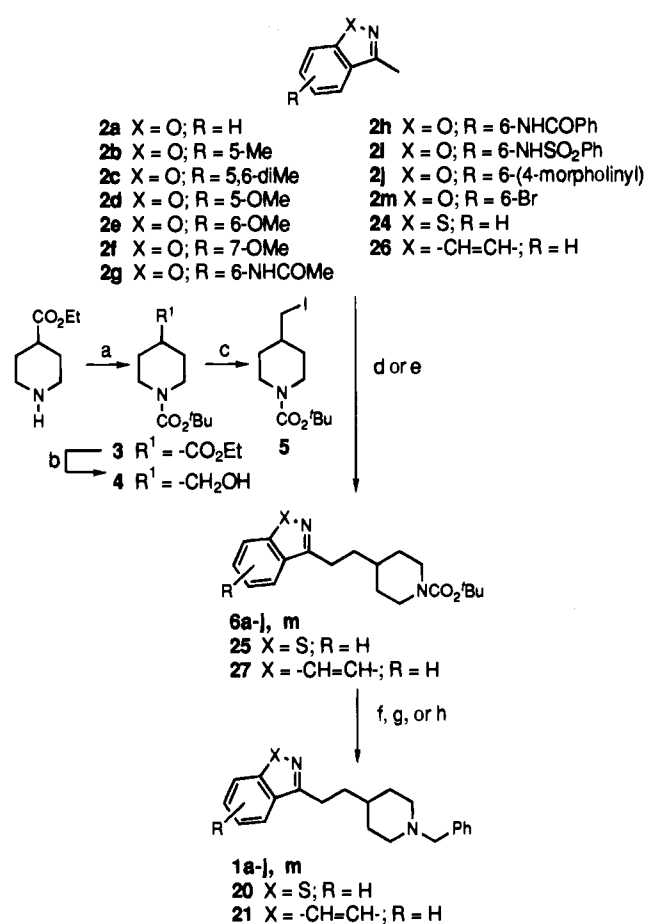
<sup>a</sup> Reagents: (a) NH<sub>2</sub>OH·HCl, NaOAc·3H<sub>2</sub>O, EtOH, H<sub>2</sub>O, reflux, 2 h; (b) Ac<sub>2</sub>O, reflux, 2 min; (c) pyr, reflux, 12 h; (d) 1 N HCl, reflux, 45 min; (e) PhCOCl, Et<sub>3</sub>N, DMAP, CH<sub>2</sub>Cl<sub>2</sub>, room temperature, 16 h; (f) PhSO<sub>2</sub>Cl, pyr, CH<sub>2</sub>Cl<sub>2</sub>, 0 °C, 1.3 h; (g) [Br(CH<sub>2</sub>)<sub>2</sub>]<sub>2</sub>O, Et(*i*-Pr)<sub>2</sub>N, PhMe, reflux, 15 h.

center at physiological pH. Our attention turned to a series of heterocyclic substitutions which resulted in the identification of the benzisoxazole ring (**1a**, Figure 1) as a suitable benzoyl bioisostere.<sup>15</sup> In this paper, we describe the synthesis, structure-activity relationships, and possible mode of binding of a series of *N*-benzylpiperidine benzisoxazoles and related derivatives. Molecular dynamics simulations are presented on a possible binding mode of *N*-benzylpiperidine benzisoxazoles to the X-ray crystal structure of AChE from *Torpedo californica*.

## Chemistry

Starting 3-methyl-1,2-benzisoxazoles **2a–m** were prepared according to the method of Thakar *et al.*<sup>16</sup> or as described in Scheme 1. Known 4-acetamido-2-hydroxyacetophenone<sup>17</sup> was converted *via* the oxime, oxime acetate, and pyridine-mediated cyclization<sup>16</sup> to the required *N*-acetyl benzisoxazole **2g**. Acid (HCl) hydrolysis of **2g** afforded aminobenzisoxazole **2k**. Treatment of **2k** with benzoyl chloride and benzenesulfonyl chloride under standard conditions yielded benzoyl and benzenesulfonyl benzisoxazoles **2h,i**, respectively. Bisalkylation of **2k** with β,β'-dibromodiethyl ether and diisopropylethylamine in toluene at 120 °C<sup>18</sup> gave the desired morpholino intermediate **2j**.

Compounds **2a–j,m** were alkylated with iodide **5** and converted to *N*-benzylpiperidine benzisoxazoles **1a–j,m** by removal of the *N*-BOC protecting group and benzylation, as described in Scheme 2. Commercially available ethyl isonipecotatate was converted to **5** in three steps. Protection of the amine functionality with di-*tert*-butyl dicarbonate (*t*-BOC anhydride) gave the desired *N*-BOC piperidine **3**. Selective reduction of the ester moiety with LiAlH<sub>4</sub> afforded primary alcohol **4** which was treated with iodine-triphenylphosphine in benzene to afford the desired iodide **5**. Alkylation of substituted 3-methyl-1,2-benzisoxazoles **2a–f,m** was accomplished by deprotonation with lithium diisopropylamide (LDA) in tetrahydrofuran at -78 °C in the presence of **5** to give **6a–f,m** (method A, Scheme 2). Deprotonation was carried out in the presence of electrophile **5** since it has been reported<sup>19</sup> that the lithiated species generated is unstable, undergoing fragmentation of the *N*-O linkage and formation of a dimeric structure. However, in the case of 3-methyl-1,2-benzisoxazoles **2g–j**, most of which

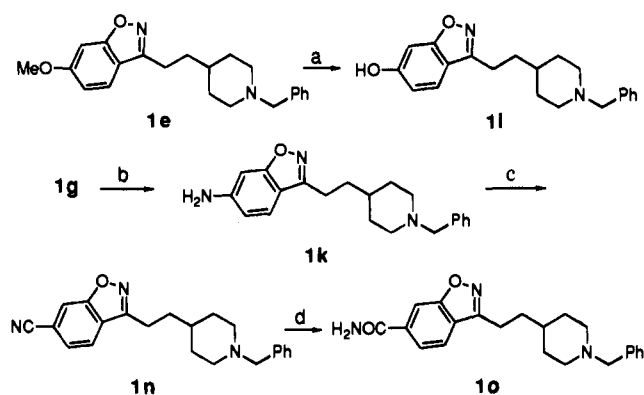
Scheme 2<sup>a</sup>

<sup>a</sup> Reagents: (a) di-*tert*-butyl dicarbonate, Et<sub>3</sub>N, 1:1 dioxane-H<sub>2</sub>O, 0 °C → room temperature, 16 h; (b) LAH, THF, 0 °C → room temperature, 16 h; (c) I<sub>2</sub>, PPh<sub>3</sub>, pyr, PhH, reflux, 1.5 h; (d) method A; (e) method B; (f) method C; (g) i. TMSOTf, 2,6-lutidine, CH<sub>2</sub>Cl<sub>2</sub>, 0 °C, 1.5 h, ii. PhCH<sub>2</sub>Br, Et<sub>3</sub>N, THF-DMF, room temperature, 24 h; (h) i. TFA, CH<sub>2</sub>Cl<sub>2</sub>, 0 °C, 30 min, ii. PhCH<sub>2</sub>Br, Na<sub>2</sub>CO<sub>3</sub>, DMF, room temperature, 2 h.

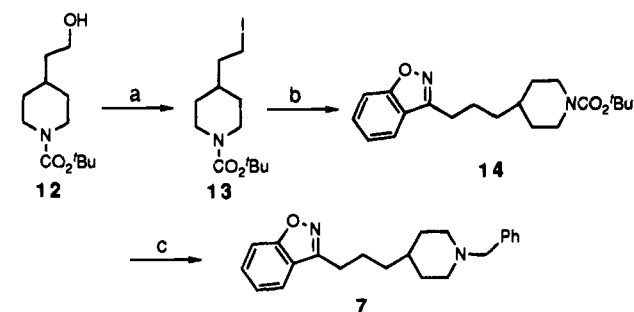
contained additional acidic protons, deprotonation was carried out first with 2 equiv of LDA in the absence of electrophile. In these cases, we found that the lithiated species generated were stable at -78 °C, undergoing smooth alkylation upon subsequent addition of electrophile **5** to afford **6g–j** (method B, Scheme 2). Removal of the *N*-BOC protecting group was accomplished by treatment with trifluoroacetic acid (method C) or trimethylsilyl trifluoromethanesulfonate and 2,6-lutidine in methylene chloride. The intermediate secondary piperidines were not isolated but submitted directly to alkylation with benzyl bromide in the presence of Et<sub>3</sub>N (method C) or Na<sub>2</sub>CO<sub>3</sub> to give **1a–j,m**. Final *N*-benzylpiperidine benzisoxazoles were isolated usually as the maleate or fumarate salts.

*N*-Benzylpiperidine benzisoxazoles **1k,l,n,o** were prepared as described in Scheme 3. Demethylation of **1e** by treatment with 48% aqueous HBr afforded hydroxybenzisoxazole **1l**. Acid (HCl) hydrolysis of acetamide **1g** gave the corresponding anilino derivative **1k**. Diazotization of **1k** with nitrous acid followed by the addition of CuCN yielded nitrile analog **1n**. Hydrolysis of **1n** with powdered KOH in *tert*-butyl alcohol<sup>20</sup> gave the primary carboxamide **1o**.

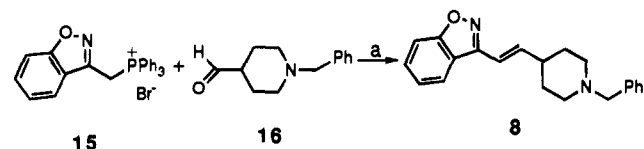
Analogues **7–11**, in which the linkage between the benzisoxazole and *N*-benzylpiperidine rings was varied,

Scheme 3<sup>a</sup>

<sup>a</sup> Reagents: (a) 48% aqueous HBr, 110 °C, 16 h; (b) 1 N HCl, reflux, 30 min; (c) aqueous HCl, NaNO<sub>2</sub>, CuCN, 0 → 50 °C, 2.5 h; (d) KOH, *t*-BuOH, 85 °C, 20 min.

Scheme 4<sup>a</sup>

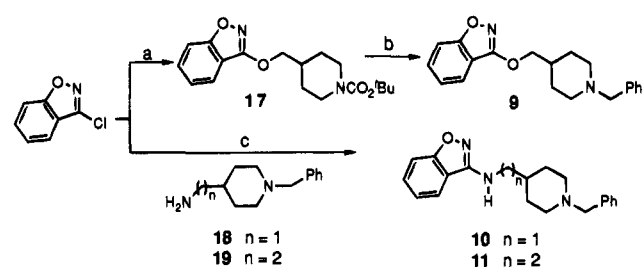
<sup>a</sup> Reagents: (a) I<sub>2</sub>, PPh<sub>3</sub>, pyr, PhH, reflux, 1.5 h; (b) method A; (c) method C.

Scheme 5<sup>a</sup>

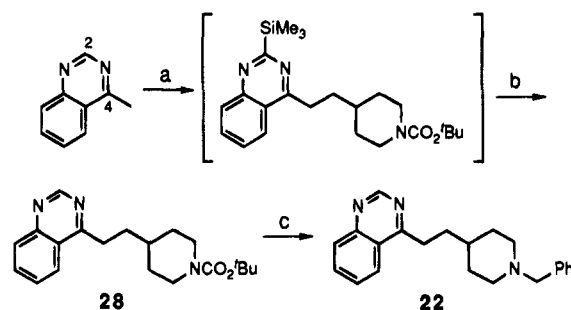
<sup>a</sup> Reagents: (a) 15, NaH, THF, room temperature, 1 h and then 16, room temperature, 4 h.

were synthesized as described in Schemes 4–6. The three-carbon analog **7** was prepared as depicted in Scheme 4. Alcohol **12**<sup>53</sup> was reacted with iodine–triphenylphosphine to give **13**. Coupling of **2a** with iodide **13** (method A) afforded N-BOC derivative **14** which was deprotected and alkylated with benzyl bromide (method C) to yield **7**. A Wittig protocol utilizing phosphonium salt **15**<sup>21</sup> and aldehyde **16**<sup>54</sup> was followed to give unsaturated analog **8** as the *E*-isomer in a stereoselective fashion (Scheme 5). Reaction of 3-chloro-1,2-benzisoxazole<sup>22</sup> with the sodium salt of alcohol **4** in dimethylformamide at 115 °C gave the corresponding N-BOC intermediate **17**, which after deprotection and alkylation (method C) resulted in desired analog **9** (Scheme 6). Compounds **10** and **11** were also obtained from 3-chloro-1,2-benzisoxazole by reaction with the corresponding known diamines **18**<sup>23</sup> and **19**<sup>13c</sup> in dimethyl sulfoxide at 150 °C.

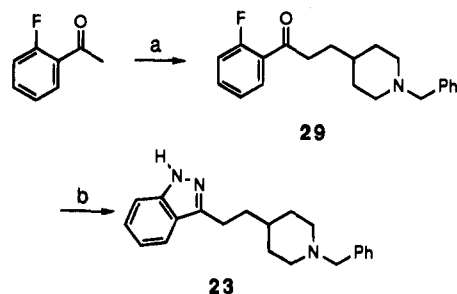
The syntheses of related heterocycles **20–23** proceeded as described below. Known 3-methyl-1,2-benzisothiazole (**24**)<sup>24</sup> and commercially available 1-methylisoquinoline (**26**) were coupled with iodide **5** (method A) to give the corresponding N-BOC derivatives **25** and **27** (Scheme 2). Deprotection and benzyl bromide alkylation (method C) then afforded the heterocyclic benz-

Scheme 6<sup>a</sup>

<sup>a</sup> Reagents: (a) **4**, NaH, DMF, 0 °C → room temperature, 10 min and then 3-chloro-1,2-benzisoxazole, 115 °C, 16 h; (b) method C; (c) **18** or **19**, K<sub>2</sub>CO<sub>3</sub>, DMSO, 150 °C, 20 h.

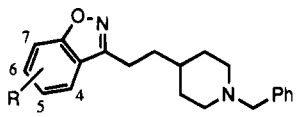
Scheme 7<sup>a</sup>

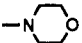
<sup>a</sup> Reagents: (a) i. 1 equiv of LDA, THF, 0 °C, ii. 1 equiv of TMSCl, 0 °C, iii. 1 equiv of LDA, THF, 0 °C, iv. **5**, 0 °C, 1 h; (b) NaOH workup; (c) method C.

Scheme 8<sup>a</sup>

<sup>a</sup> Reagents: (a) i. LHMDs, THF, -78 → -20 °C, 1 h and then **16**, -78 °C → room temperature, 40 min, ii. H<sub>2</sub>, PtO<sub>2</sub>, EtOH, 48 psi, room temperature, 2 h; (b) anhydrous NH<sub>2</sub>NH<sub>2</sub>, reflux, 3 h.

isothiazole and isoquinoline analogs **20** and **21**, respectively. Attempts to synthesize quinazoline and indazole analogs **22** and **23** under similar conditions were unsuccessful. Deprotonation of 4-methylquinazoline with LDA (1–3 equiv) in the presence of or followed by the addition of iodo compound **5** resulted only in recovered starting material or decomposition. After some experimentation, a successful one-pot protocol was developed (Scheme 7) which involved sequential addition of 1 equiv of LDA, trimethylsilyl chloride (to react with anion at carbon-two), a second equivalent of LDA, and iodide **5**. The silyl group was removed upon workup with base to give the corresponding N-BOC intermediate **28** which was deprotected and alkylated (method C) to afford **22**. Indazole **23** was synthesized by a sequence utilizing a different bond disconnection (Scheme 8).<sup>25</sup> Condensation of *o*-fluoroacetophenone with piperidine aldehyde **16**<sup>54</sup> was followed by hydrogenation of the resulting olefin with PtO<sub>2</sub> to afford ketone **29**. Reaction of **29** with anhydrous hydrazine resulted in formation of the corresponding hydrazone which underwent cyclization and elimination of HF *in situ* to provide indazole **23**.

**Table 1.** *In Vitro* Inhibition of AChE<sup>a</sup> by Benzisoxazole Derivatives **1a–o** and E-2020


compd no.	R	IC <sub>50</sub> (nM) <sup>b</sup>
<b>1a</b>	H	55 ± 12
<b>1b</b>	5-Me	7.8 ± 3.5
<b>1c</b>	5,6-diMe	5.8 ± 4.0
<b>1d</b>	5-OMe	7.2 ± 3.2
<b>1e</b>	6-OMe	8.3 ± 2.7
<b>1f</b>	7-OMe	7.1 ± 3.0
<b>1g</b>	6-NHCOMe	2.8 ± 2.2
<b>1h</b>	6-NHCOPh	9.4 ± 4.8
<b>1i</b>	6-NHSO <sub>2</sub> Ph	14 ± 2.3
<b>1j</b>	6- 	0.80 ± 0.3
<b>1k</b>	6-NH <sub>2</sub>	20 ± 3.8
<b>1l</b>	6-OH	26 ± 4.4
<b>1m</b>	6-Br	50 ± 4.7
<b>1n</b>	6-CN	101 ± 49
<b>1o</b>	6-CONH <sub>2</sub>	8.8 ± 2.4
E-2020		8.0 ± 3.4

<sup>a</sup> Source of AChE: human erythrocytes. <sup>b</sup> IC<sub>50</sub> values are the mean ± standard deviation of three assays.

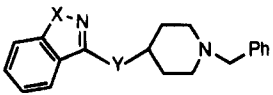
### Structure–Activity Relationships

The benzisoxazoles and structurally related compounds were evaluated *in vitro* for inhibition of AChE by the spectroscopic method of Ellman *et al.*<sup>26</sup> The results are presented in Tables 1 and 2.

Substitution of the benzisoxazole ring with electron-donating and some electron-withdrawing groups resulted in an increase of AChE inhibition in comparison to the unsubstituted compound **1a** (Table 1). Nitrogen-containing functionalities such as cyclic amines and *N*-acyl groups at position 6 were particularly interesting, resulting in a 3–100-fold increase in the inhibition of AChE in comparison to other alkyl, alkoxy, or electron-withdrawing groups. The 6-morpholino and 6-NHAc analogs **1j,g**, respectively, displayed potent inhibition in the low nanomolar range (IC<sub>50</sub>'s = 0.8–3.0 nM). The 6-OH and 6-NH<sub>2</sub> derivatives were less potent than the corresponding alkylated or acylated derivatives, suggesting a preference for lipophilic substituents. This preference is also reflected on the lower potency displayed by the sulfonamide analog **1i**. In general, among the benzisoxazole substituents studied, inhibition of AChE seemed independent of steric factors but was influenced by lipophilicity.

The two-carbon methylene bridge between the benzisoxazole and piperidine rings was optimum. The length of the bridge and the freedom of rotation around the two-atom connecting unit played a significant role in the ability of these compounds to inhibit AChE. A three-carbon chain (**7**) led to a substantial (16-fold) loss of activity (Table 2). Restricting rotation by introduction of a double bond (**8**, *E* configuration) resulted in a 4-fold decrease in inhibition. Diminished inhibition of AChE was also observed after introduction of heteroatoms such as oxygen or nitrogen (**9–11**).

Heterocyclic systems structurally related to the benzisoxazole nucleus were prepared and evaluated for inhibition of AChE. The closely related benzisothiazole (**20**) and indazole (**23**) derivatives were 3–4 times less potent than **1a** (Table 2). Such a difference between the oxygen- and sulfur-containing heterocycles is re-

**Table 2.** *In Vitro* Inhibition of AChE<sup>a</sup> for Benzisoxazole Derivatives with Different Spacing Units (-Y-) and Related Heterocycles (-X-)


compd no.	-X-	-Y-	IC <sub>50</sub> (μM) <sup>b</sup>
<b>7</b>	-O-	-(CH <sub>2</sub> ) <sub>3</sub> -	0.90 ± 0.18
<b>8</b>	-O-	<i>E</i> -CH=CH-	0.21 ± 0.03
<b>9</b>	-O-	-OCH <sub>2</sub> -	2.6 ± 0.30
<b>10</b>	-O-	-NHCH <sub>2</sub> -	0.32 ± 0.20
<b>11</b>	-O-	-NH(CH <sub>2</sub> ) <sub>2</sub> -	0.81 ± 0.02
<b>20</b>	-S-	-(CH <sub>2</sub> ) <sub>2</sub> -	0.099 ± 0.009
<b>21</b>	-CH=CH-	-(CH <sub>2</sub> ) <sub>2</sub> -	0.22 ± 0.05
<b>22</b>	-N=CH-	-(CH <sub>2</sub> ) <sub>2</sub> -	0.34 ± 0.07
<b>23</b>	-NH-	-(CH <sub>2</sub> ) <sub>2</sub> -	0.12 ± 0.02

<sup>a</sup> Source of AChE: human erythrocytes. <sup>b</sup> IC<sub>50</sub> values are the mean ± standard deviation of three assays.

**Table 3.** Comparison of the *in Vitro* Selectivity for AChE<sup>a</sup> over BuChE<sup>b</sup> for Selected Benzisoxazole Derivatives and Known AChE Inhibitors

compd	IC <sub>50</sub> (nM) <sup>c</sup>		ratio BuChE/AChE
	AChE	BuChE	
<b>1g</b>	2.8 ± 2.2	9000 ± 300	3200
<b>1j</b>	0.8 ± 0.3	4700 ± 1000	5900
E-2020	8.0 ± 3.4	2900 ± 60	360
THA	270 ± 140	6.0 ± 0.1	0.022
physostigmine	19 ± 5.0	73 ± 6.0	3.8

<sup>a</sup> Source of AChE: human erythrocytes. <sup>b</sup> Source of BuChE: horse serum. <sup>c</sup> IC<sub>50</sub> values are the mean ± standard deviation of three assays.

markable and indicative of the specific hydrogen-bonding requirements of the enzyme. The larger heterocyclic derivatives, isoquinoline **21** and quinazoline **22**, were also less potent.

### Biological Results and Discussion

The *N*-benzylpiperidine benzisoxazoles **1b–j,o** displayed potent *in vitro* inhibition of AChE comparable to or better than E-2020. As mentioned above, *N*-acetyl derivative **1g** and morpholino derivative **1j** were among the most potent compounds in this new class of inhibitors. In addition, these compounds showed outstanding selectivity for acetyl- over butyrylcholinesterase (BuChE) as demonstrated by ratios in excess of 3 orders of magnitude (Table 3). While E-2020 also displayed good selectivity (300-fold), THA and physostigmine showed poor selectivity for the cholinesterases. Inhibition of BuChE, which is abundant in plasma, may be associated with potentiating peripheral side effects.<sup>27</sup> Therefore, an inhibitor which is essentially devoid of BuChE activity may display higher therapeutic indices.

*In vivo* activity was studied by measuring elevation of whole brain ACh in mouse forebrain in a selected number of compounds. *N*-Acetyl **1g** displayed the best profile with an ED<sub>50</sub> of 2.4 mg/kg, po (Figure 2). A dose-dependent elevation of ACh was measured at 0.32–100 mg/kg with a maximum elevation of 178%. Acute (1 h) LD<sub>50</sub> was greater than 100 mg/kg. E-2020 and THA produced a similar maximum elevation of ACh (160%) but were less potent with ED<sub>50</sub>'s of 14 mg/kg (Figure 2).

Compound **1g** was also assessed in a mouse passive avoidance model for its ability to reverse hemicholinium-3-induced amnesia. At doses of 3.2 and 5.6 mg/kg, **1g**

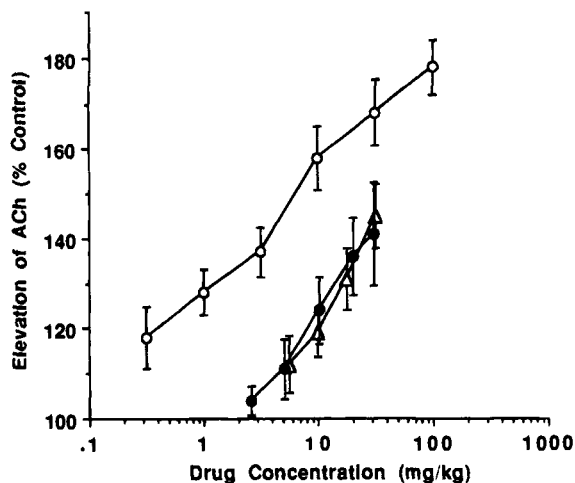


**Figure 2.** Elevation of acetylcholine in mouse forebrain following oral administration. Refer to the Experimental Section for test procedures. Compounds shown: **1g** (○), THA (△), and E-2020 (●).

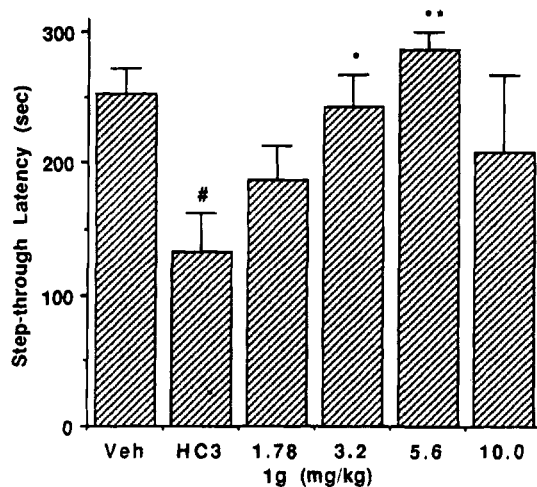


**Figure 3.** Mouse passive avoidance test: reversal of hemicholinium-3 (HC3)-induced amnesia after oral administration. Veh = vehicle. Mann-Whitney *U* test: # =  $p < 0.05$  vs vehicle treated; \* =  $p < 0.05$  and \*\* =  $p < 0.01$  vs HC3 treated. Refer to the Experimental Section for test procedures.

was able to reverse amnesia efficiently, with an average reversal of 89.7% (Figure 3). THA also reversed amnesia at the higher dose of 32 mg/kg (data not shown).

### Model Binding Mode

The publication by Sussman *et al.*<sup>28</sup> of the X-ray structure of AChE from *T. californica* prompted us to investigate the possible binding modes of our potent benzisoxazole inhibitors. Molecular dynamics simulations were carried out as described in the Computational Methods section utilizing benzisoxazole **1g** as the model inhibitor.

The results of the simulations allowed identification of the key features of the benzisoxazole class of inhibitors that are responsible for their high potency. The key interactions are illustrated in Figure 4. For inhibitor **1g**, there are five possible hydrogen-bonding sites available: the protonated piperidine N—H, the benzisoxazole nitrogen and oxygen, and the acetyl N—H and carbonyl oxygen. Arguably the most critical interaction is formed between the positively charged piperidine of **1g** and the negatively charged carboxylate side chain of Asp-72. This hydrogen bond is present 90% of the time and

forms the foundation upon which the remaining contacts rest. Examination of the native X-ray structure reveals that the carboxylate of Asp-72 is hydrogen bonded to the hydroxyl group of Tyr-334 and presumably hydrated with solvent, though no crystallographic water molecules are observed in this region. During the simulation, the hydrogen bond between the carboxylate of Asp-72 and the phenol OH of Tyr-334 remains intact. The rigidity of this arrangement further serves to anchor the location of the piperidine within the gorge. In general, there is little change observed in the structure of the protein throughout the course of the simulation, though there are notable exceptions (*vide infra*).

Another frequently observed (93% of the time) hydrogen bond is the one between the benzisoxazole oxygen of **1g** and the backbone N—H of Phe-288, which is found on the floor of the gorge. This backbone N—H also participates in forming a hydrogen bond with the benzisoxazole nitrogen 40% of the time. As one would expect, if the complementary hydrogen-bonding sites on the benzisoxazole are replaced with weak hydrogen-bond acceptors, or are removed completely (*cf.* Table 2, compounds **20–22**), there is a significant decrease in the potency of the inhibitors. The decrease in potency is consistent with the binding mode determined from the simulation. Since the backbone N—H of Phe-288 will be hydrated in the absence of an inhibitor, failure to replace this interaction with a complementary site on the inhibitor will result in deleterious binding.

The acetyl substituent of **1g** is primarily solvent exposed and does not appear to engage in specific hydrogen-bonding interactions with the protein, *per se*. A hydrogen bond between the amide N—H of **1g** and the carbonyl oxygen of Gly-335 is observed during the initial phases of the simulation, but this interaction ultimately yields to a water bridge that is formed between the carbonyl oxygen of the acetyl group and the carboxylate group of Asp-285.

Hydrophobic interactions are also evident for the enzyme–inhibitor model. Indeed, the gorge leading to the active site is lined with aromatic residues, which constitute *ca.* 40% of the residues present in this region.<sup>28</sup> Inhibitor **1g** takes advantage of this hydrophobic lining by making a variety of specific and nonspecific contacts. The *N*-benzyl substituent of **1g** forms an off-center  $\pi$ -stacking interaction with the indole side chain of Trp-84. The arrangement of the rings is roughly parallel with the centers displaced such that the edge of the phenyl ring slightly overlaps the edge of the indole formed by the atoms CG—CD2—CE3 (Figure 4). It is noteworthy that the average center-to-center distance between the plane of the indole and the benzyl rings of Trp-84 and **1g**, respectively, is 5.1 Å, as computed from the coordinates of the saved configurations. This distance is near the minimum (4.5 Å) reported for a planar  $\pi$ -stacked interaction between two benzene rings in the gas phase, with a similar off-center geometry.<sup>29</sup> Trp-84 has been implicated in the binding of acetylcholine and other quaternary ligands.<sup>28,30</sup> As other studies have reported,<sup>30</sup> we find little change in the position of the side chain of Trp-84 during the simulation. In fact, the average  $\chi_1$  torsion measured from the simulation is  $-59^\circ$ , compared to the X-ray value of  $-46^\circ$ , while  $\chi_2$  changes by less than  $1^\circ$ . In addition to the important interaction of Trp-84 with the

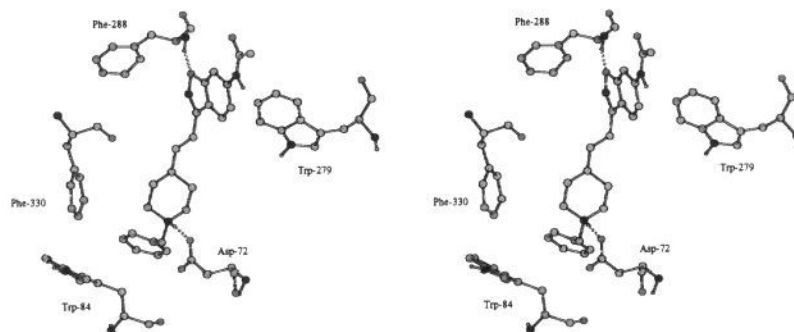


**Figure 4.** Stereoplot of inhibitor **1g** bound within the active site gorge of acetylcholinesterase. Coordinates were obtained from an instantaneous structure generated during the MD simulation (100 ps). Hydrogen bonds are indicated with dashed lines.

*N*-benzyl substituent of **1g**, we find that the phenyl ring of Phe-330 interacts with the phenyl ring of **1g** via an edge-on configuration.<sup>29</sup> Again averaging over the saved coordinates, we find the average center-to-center distance between the two phenyl rings is computed to be 6.4 Å. While this distance is larger than optimal (5.0 Å reported for the T-shaped interaction in the gas phase), the interaction of the benzyl substituent with the hydrophobic pocket formed by the side chains of Trp-84 and Phe-330 undoubtedly contributes greatly to the potency of this class of inhibitors. Also evident from Figure 4 is the close packing of the piperidine ring with the phenyl group of Phe-330. Unlike the previously described interaction with Trp-84, we note the side chain of Phe-330 differs significantly from the orientation reported in the "native" X-ray structure. Upon binding inhibitor **1g**, the plane of the phenyl ring rotates about the  $\chi_2$  torsion *ca.* 113°, affording greater contacts with not only the benzyl group but the piperidine ring as well. Some caution is warranted in drawing any conclusions about the relative rotations in Phe-330 since the "native" X-ray structure has been reported to contain complexed decamethonium, which has been shown to bind in this region.

Changing the length of the chain that connects the piperidine to the benzisoxazole substituent has been shown to have a profound effect on the potency (*cf.* Table 2, compound **7**). The optimal length ethyl spacer (*i.e.*, **1g**) is completely consistent with our proposed binding model. Since the *N*-benzylpiperidine fragment is ideally situated, the nature of the spacer will control the positioning of the benzisoxazole within the gorge and hence the extent of contact with the protein. The indole side chain of Trp-279, which is located near the rim of the gorge, forms an edge-to-face contact pair with the benzisoxazole (average distance of 5.7 Å). In order to form this contact, the  $\chi_1$  and  $\chi_2$  angles of Trp-279 are rotated by *ca.* -30° and 60°, respectively, relative to the X-ray structure. The excellent complementarity between the narrow gorge of the protein and the inhibitor is illustrated in Figure 5. Examination of Table 2 reveals a 16-fold decrease in activity on going from the ethyl to propyl linker. We can rationalize this result by realizing that the propyl spacer of **7** would force the benzisoxazole substituent out of the gorge and preclude, or at the very least reduce, its interaction with the protein. On the other hand, shortening the spacer would have the same effect of forcing the benzisoxazole

away from the protein and would disrupt potential hydrogen-bonding and hydrophobic interactions.

A potential source of difficulty in attempting to rationalize all of the *in vitro* binding data comes from the fact that we are studying the possible binding modes of **1g** to AChE from *T. californica* while the *in vitro* binding studies were conducted with human AChE. Clearly, there are likely to be subtle differences in the binding modes caused by differences in the structures between these two AChE. However, we note that in the sequence of human AChE,<sup>31</sup> Asp-72, Trp-84, Trp-279, Phe-288, and Phe-330 are conserved while Asp-285 in *T. californica* AChE has been replaced by Glu in the human sequence. Since Asp-285 is located on the outer rim of the gorge, and is completely solvent exposed, mutating this to Glu would likely have minor effects on the binding of **1g** and other inhibitors of this class.

## Conclusions

A novel series of benzisoxazoles has been synthesized and found to be potent and selective inhibitors of AChE *in vitro*. The benzisoxazole heterocycle was found to be a suitable bioisosteric replacement for the benzoyl moiety present in the *N*-benzylpiperidine class of inhibitors. In addition, these compounds are devoid of chiral centers, existing as pure chemical entities at physiological pH. Substitution at position 6 with nitrogen-containing groups resulted in optimization of *in vitro* activity. The benzisoxazoles displayed favorable *in vivo* profiles as demonstrated by the dose-dependent elevation of ACh in mouse forebrain and reversal of amnesia in a passive avoidance model. A model for the binding of this class of inhibitors to AChE (from *T. californica*) is proposed which is consistent with the available structure-activity relationships. The potency of the inhibitors is derived from the many hydrogen bonds and aromatic contacts that are made with the enzyme. The *N*-benzylpiperidine benzisoxazoles may be suitable compounds for the palliative treatment of Alzheimer's Disease.

## Experimental Section

**Computational Methods.** Molecular dynamics simulations were carried out using the AMBER 4.0 series of programs<sup>32</sup> on a Silicon Graphics Iris-4D computer. The standard OPLS parameters were used for the protein,<sup>33</sup> modified to incorporate all-atom parameters for the aromatic rings.<sup>29</sup> The TIP3P model for water<sup>34</sup> was used to describe the solvent.

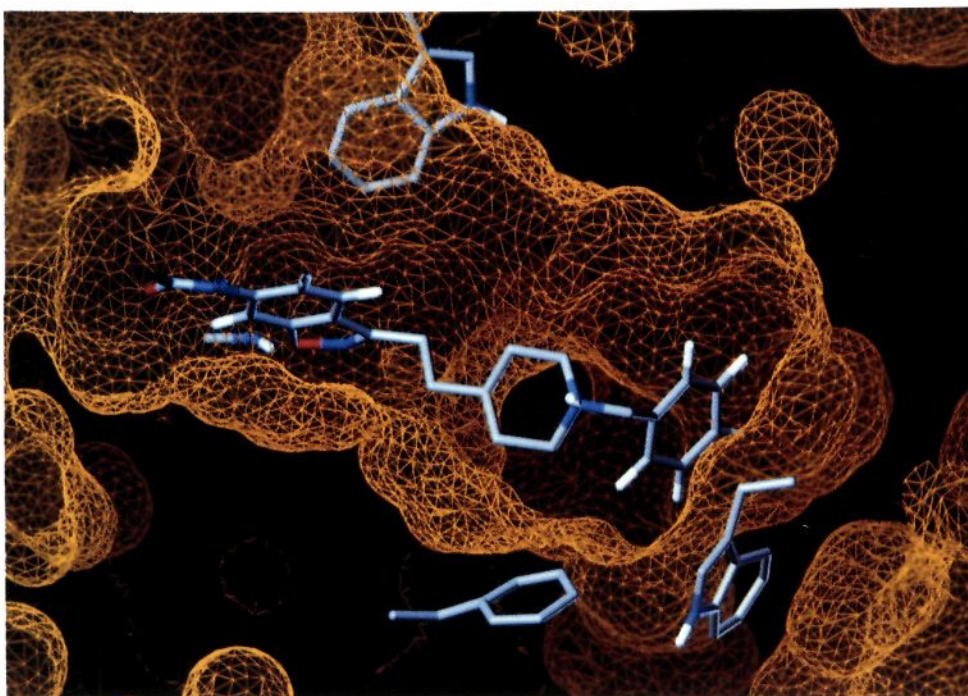


**Figure 5.** Inhibitor **1g** bound, demonstrating the complementary fit with the enzyme. The solvent accessible surface is depicted in wireframe, generated with the SYBYL program.<sup>48</sup>

Parameters for inhibitor **1g** were derived following the OPLS paradigm; standard Lennard–Jones  $\sigma$  and  $\epsilon$  values that are consistent with atomic hybridization were employed, while partial atomic charges were varied in order to obtain high quality parameters. Ideally, these charges would be optimized by fitting the results of fluid simulations to experimental data on pure liquids or dilute aqueous solutions.<sup>35</sup> In the absence of such data, one method of charge assignment, which has shown excellent success, is to merge the partial charges from readily available fragments.<sup>36,37</sup> In the case of inhibitor **1g**, OPLS parameters for the benzyl,<sup>36</sup> piperidine,<sup>38</sup> alkyl,<sup>39</sup> and acetamide<sup>33</sup> fragments have been previously reported. As is usual, aromatic rings were represented by an all-atom model, while the aliphatic portions were given by united-atom models.

Partial atomic charges for the benzisoxazole substituent were determined by fitting, *via* the CHELPG program,<sup>40</sup> to the electrostatic potential surface (EPS) computed from the Hartree–Fock 6-31G(d)<sup>41a</sup> wave function. The geometry for benzisoxazole was first fully optimized by means of analytical energy gradients<sup>42</sup> at the restricted Hartree–Fock level of theory with the 3-21G<sup>41b</sup> basis set. The *ab initio* molecular orbital calculations were carried out with the Gaussian92 series of programs.<sup>43</sup> Jorgensen and co-workers have found that charges derived from fitting to the EPS from 6-31G(d) wave functions yield results similar in quality and consistency to those derived from more elaborate methodologies.<sup>44</sup> This “hybrid” approach of merging OPLS- and EPS-derived charges has been recommended in the case of systems containing alkyl and amide fragments, due to significant errors in the computed free energies of hydration, as described in detail elsewhere.<sup>44</sup> Parameters used to compute the angle bending and torsional motion, including improper torsions, were taken from the AMBER force field.<sup>45</sup> Full parameter specifications for **1g** are given in the supplementary material.

Scaling factors for the 1,4-nonbonded interactions were set as specified in the OPLS description.<sup>33</sup> The SHAKE algorithm,<sup>46</sup> with a tolerance of 0.0004 Å, was used to constrain all bonds involving hydrogens at their equilibrium values. A 9 Å residue-based cutoff was applied to all nonbonded interactions, which were generated using a pair list that was updated every 25 steps. A 1.5 fs time step was used throughout the molecular dynamics simulations.

The coordinates of the protein were obtained from the X-ray structure of AChE isolated from *T. californica*,<sup>28</sup> as deposited in the Brookhaven Protein Data Bank (entry 1ACE).<sup>47</sup> Crystallographic water molecules present in the X-ray structure as well as a modeled acetylcholine molecule were deleted. Polar and aromatic hydrogen atoms, in addition to any missing heavy atoms, were added to the protein using the SYBYL program.<sup>48</sup> Initial docking of **1g** within the gorge leading to the active site was accomplished by locating possible salt bridge and hydrogen-bonding sites on the protein that could complement those found on the inhibitor. Of the four negatively charged amino acids lining the gorge of the active site, only Asp-72 afforded the accessibility necessary to interact with the positively charged piperidine of **1g**. This key interaction formed the essential anchoring point and was used to guide the initial placement of **1g** within the gorge that leads to the active site. The inhibitor was placed in the gorge with the piperidine N–H oriented in a roughly perpendicular fashion to the plane formed by the carboxylate group of Asp-72 *ca.* 1.8 Å away. The benzyl and benzisoxazole substituents were rotated into the gorge such that unfavorable van der Waals contacts were avoided. The narrow gorge does not allow a large number of choices in this regard, which makes positioning the substituents considerably easier than may otherwise be expected. Several alternative orientations were explored; none were consistent with the available SAR and high potency/selectivity of **1g** toward AChE (*vide infra*). The initial placement of **1g** is also consistent with the results of an independent docking study of E-2020 within the gorge.<sup>49</sup> A 25 Å sphere of TIP3P water was centered on the side chain carboxylate carbon of Asp-72, and all water molecules within 1.7 Å of any protein or inhibitor atom were removed. A simple harmonic potential function with a force constant of 1.5 kcal/(mol Å<sup>2</sup>) was used to maintain the spherical boundary of the solvent.

The initial system was equilibrated in several phases. Initially, 5000 steps of the steepest descent minimization was performed on the water molecules while keeping the protein and inhibitor fixed, followed by 15 ps of MD at 200 K. Next, 30 ps of equilibration was carried out while allowing the water, inhibitor, and all protein residues within 20 Å of the center of the sphere of water to move. During this phase, the tempera-

ture of the system was raised to 298 K. Since some relaxation of the protein allows pockets to form, resolution of the system becomes advantageous to ensure an adequately packed environment. The above system was resolvated by adding additional water (as above), bringing the total number of water molecules present to 1247. Finally, another 50 ps of equilibration at 298 K was carried out to ensure a stable system before any data collection was begun. Data collection was then carried out during a 210 ps constant temperature simulation in which coordinates were saved every 50 steps. Hydrogen-bonding analysis was performed on the saved coordinate sets from the simulations. In defining hydrogen bonds, a purely geometric criterion was applied. A hydrogen bond was considered to exist if the hydrogen-acceptor distance was less than 2.5 Å and the donor-hydrogen-acceptor angle was between 120° and 180°.

**General Procedures.** Melting points were determined in a Thomas-Hoover or Electrothermal capillary melting point apparatus and are uncorrected. High-field  $^1\text{H-NMR}$  spectra were recorded on a Bruker AM 250, Bruker AM 300, or Varian XL-300 instrument. Low- and high-resolution electron impact mass spectra (EIMS and EIHRMS) were recorded in a Kratos Profile instrument. Low- and high-resolution fast-atom bombardment mass spectra (FABMS and FABHRMS) were recorded in a Kratos Concept instrument. Low-resolution chemical ionization spectra (CIMS) were recorded in a Hewlett-Packard 5989A instrument. Elemental analysis were carried out by Mr. J. W. Greene, Analytical Department, Pfizer Inc., or Schwarzkopf Microanalytical, Woodside, NY. Flash chromatography was performed on EM Kieselgel 60 (40–60  $\mu\text{m}$ , 230–400 mesh).

All reactions were carried out under a positive pressure of nitrogen, unless otherwise noted. Tetrahydrofuran (THF) and dimethoxyethane (DME) were distilled immediately before use from sodium benzophenone ketyl. Anhydrous methylene chloride ( $\text{CH}_2\text{Cl}_2$ ), dimethylformamide (DMF), dimethyl sulfoxide (DMSO), and toluene were purchased from Aldrich Chemical Co. 3-Methyl-1,2-benzisoxazole (**2a**),<sup>16</sup> 3,5-dimethyl-1,2-benzisoxazole (**2b**),<sup>16</sup> 3,5,6-trimethyl-1,2-benzisoxazole (**2c**),<sup>16</sup> 5-methoxy-3-methyl-1,2-benzisoxazole (**2d**),<sup>50</sup> 6-methoxy-3-methyl-1,2-benzisoxazole (**2e**),<sup>51</sup> 7-methoxy-3-methyl-1,2-benzisoxazole (**2f**),<sup>52</sup> and 6-bromo-3-methyl-1,2-benzisoxazole (**2m**)<sup>16</sup> are known and were prepared by the method of Thakar *et al.*<sup>16</sup> from the corresponding *o*-hydroxyacetophenones.

**6-Acetamido-3-methyl-1,2-benzisoxazole (2g).** A solution of hydroxylamine hydrochloride (6.14 g, 0.088 mol) and sodium acetate trihydrate (12.6 g, 0.092 mol) dissolved in the minimum amount of 7:3 EtOH–H<sub>2</sub>O was added to a solution of 4-acetamido-2-hydroxyacetophenone<sup>53</sup> (14.85 g, 0.077 mol) in 7:3 EtOH–H<sub>2</sub>O (100 mL). The resulting mixture was heated to reflux. After 1.5 h, additional hydroxylamine hydrochloride (2.70 g, 0.038 mol) and sodium acetate trihydrate (5.23 g, 0.038 mol) dissolved in the minimum amount of water were added. Reflux was continued for 0.5 h. The reaction mixture was concentrated, and the solid obtained was collected by filtration. After washing with water and drying under high vacuum, 11.37 g (71%) of the oxime was obtained as a light tan solid: mp (EtOAc) 200–202.5 °C;  $^1\text{H-NMR}$  (DMSO-*d*<sub>6</sub>)  $\delta$  11.66 (s, 1H), 11.37 (s, 1H), 9.97 (s, 1H), 7.38 (d, 1H,  $J = 8.5$  Hz), 7.23 (d, 1H,  $J = 1.6$  Hz), 7.03 (dd, 1H,  $J = 8.6$  Hz,  $J = 1.6$  Hz); EIMS  $m/e$  (rel intensity) 208 ( $\text{M}^+$ , 100). Anal. ( $\text{C}_{10}\text{H}_{12}\text{N}_2\text{O}_3$ ) C, H, N.

Acetic anhydride (28.5 mL) was added to the oxime (11.3 g, 0.054 mol) obtained above, and the mixture was heated at 130 °C for 2 min. After allowing to cool to room temperature, the reaction mixture was filtered. The off-white solid collected was washed with H<sub>2</sub>O and dried under high vacuum to yield 11.35 g (83%) of the oxime acetate: mp (EtOAc) 178–179 °C;  $^1\text{H-NMR}$  (DMSO-*d*<sub>6</sub>)  $\delta$  11.03 (s, 1H), 10.08 (s, 1H), 7.46 (d, 1H,  $J = 8.6$  Hz), 7.38 (d, 1H,  $J = 2.0$  Hz), 7.07 (dd, 1H,  $J = 8.6$  Hz,  $J = 2.0$  Hz), 2.38 (s, 3H), 2.22 (s, 3H), 2.06 (s, 3H); EIMS  $m/e$  (rel intensity) 250 ( $\text{M}^+$ , 11), 148 (100). Anal. ( $\text{C}_{12}\text{H}_{14}\text{N}_2\text{O}_4$ ) C, H, N.

The above oxime acetate (11.3 g, 0.045 mol) was dissolved in pyridine (100 mL), and the mixture obtained was heated to reflux for 12 h. The reaction mixture was allowed to cool to

room temperature and poured over 1 N HCl. The aqueous layer was extracted with ethyl acetate (3 $\times$ ), and the combined organic layer was washed with additional 1 N HCl and brine, dried ( $\text{MgSO}_4$ ), filtered, and concentrated. Purification by silica gel flash chromatography (50% → 100% ethyl acetate–hexanes) gave **2g** (5.33 g, 62%) as a white solid: mp (EtOAc/hexanes) 210–211 °C;  $^1\text{H-NMR}$  (DMSO-*d*<sub>6</sub>)  $\delta$  10.36 (s, 1H), 8.14 (d, 1H,  $J = 1.2$  Hz), 7.72 (d, 1H,  $J = 8.6$  Hz), 7.35 (dd, 1H,  $J = 8.6$  Hz,  $J = 1.6$  Hz), 2.49 (s, 3H), 2.10 (s, 3H); EIMS  $m/e$  (rel intensity) 190 ( $\text{M}^+$ , 79), 148 (100). Anal. ( $\text{C}_{10}\text{H}_{10}\text{N}_2\text{O}_2$ ) C, H, N.

**6-Amino-3-methyl-1,2-benzisoxazole (2k).** A mixture of **2g** (1.07 g, 5.63 mmol) in 1 N HCl (20 mL) was heated to reflux until a clear solution was obtained (45 min). The mixture was allowed to cool to room temperature and made basic by addition of 10% NaOH. The off-white solid obtained was collected by filtration, washed with H<sub>2</sub>O, and dried under high vacuum to give 0.619 g (74%) of **2k**: mp (Et<sub>2</sub>O) 118–120 °C;  $^1\text{H-NMR}$  ( $\text{CDCl}_3$ )  $\delta$  7.38 (d, 1H,  $J = 8.5$  Hz), 6.61 (dd, 1H,  $J = 8.5$  Hz,  $J = 1.7$  Hz), 6.57 (d, 1H,  $J = 1.5$  Hz), 2.37 (s, 3H); EIMS  $m/e$  (rel intensity) 148 ( $\text{M}^+$ , 100); EIHRMS calcd for  $\text{C}_8\text{H}_8\text{N}_2\text{O}$  148.0637, found 148.0619. Anal. ( $\text{C}_8\text{H}_8\text{N}_2\text{O}$ ) C, H, N: calcd, 18.91; found, 18.46.

**6-Benzamido-3-methyl-1,2-benzisoxazole (2h).** Benzoyl chloride (0.56 mL, 4.82 mmol) was added to a solution of **2k** (0.70 g, 4.72 mmol), triethylamine (1.35 mL, 9.69 mmol), and 4-(dimethylamino)pyridine (0.07 g, 0.57 mmol) in  $\text{CH}_2\text{Cl}_2$ . The resulting mixture was stirred overnight at room temperature. The heterogenous mixture was concentrated, and the solid obtained was collected, washed with H<sub>2</sub>O and Et<sub>2</sub>O, and air-dried to give **2h** (1.02 g, 86%) as an off-white solid. A small sample was purified by recrystallization from EtOH to give a white solid: mp (EtOH) 213–214 °C;  $^1\text{H-NMR}$  (DMSO-*d*<sub>6</sub>)  $\delta$  10.6 (s, 1H), 8.30 (s, 1H), 7.98 (d, 2H,  $J = 6.9$  Hz), 7.80 (d, 1H,  $J = 8.6$  Hz), 7.68 (d, 1H,  $J = 8.8$  Hz), 7.52–7.63 (m, 3H), 2.53 (s, 3H); EIMS  $m/e$  (rel intensity) 252 ( $\text{M}^+$ , 17), 105 (100). Anal. ( $\text{C}_{15}\text{H}_{12}\text{N}_2\text{O}_2$ ) C, H, N.

**6-Benzenesulfonamido-3-methyl-1,2-benzisoxazole (2i).** Benzenesulfonyl chloride (0.528 mL, 4.14 mmol) was added to a cold (0 °C) solution of **2k** (0.613 g, 4.14 mmol) and pyridine (0.670 mL, 8.28 mmol) in  $\text{CH}_2\text{Cl}_2$  (30 mL). After 1.3 h, saturated  $\text{NaHCO}_3$  was added and the resulting mixture was stirred overnight at room temperature. The organic layer was separated, washed with H<sub>2</sub>O and brine, dried ( $\text{MgSO}_4$ ), filtered, and concentrated. Purification by silica gel flash chromatography (5% EtOAc– $\text{CH}_2\text{Cl}_2$ ) gave **2i** (0.867 g, 83%) as a white solid: mp 183–184 °C;  $^1\text{H-NMR}$  ( $\text{CDCl}_3$ )  $\delta$  10.9 (br s, 1H), 7.84 (d, 2H,  $J = 6.7$  Hz), 7.68 (d, 1H,  $J = 8.5$  Hz), 7.52–7.63 (m, 3H), 7.34 (d, 1H,  $J = 1.5$  Hz), 7.11 (dd, 1H,  $J = 8.5$  Hz,  $J = 1.7$  Hz), 2.52 (s, 3H); EIMS  $m/e$  (rel intensity) 288 ( $\text{M}^+$ , 46), 147 (100). Anal. ( $\text{C}_{14}\text{H}_{12}\text{N}_2\text{O}_3\text{S}$ ) C, H, N.

**3-Methyl-6-(4-morpholinyl)-1,2-benzisoxazole (2j).** A mixture of **2k** (0.230 g, 1.55 mmol),  $\beta,\beta'$ -dibromodiethyl ether (0.397 g, 1.71 mmol), and diisopropylethylamine (Hunig's base, 0.648 mL, 3.72 mmol) in toluene (2.5 mL) was heated at 120 °C for 15 h. The cooled reaction mixture was diluted with EtOAc, washed with H<sub>2</sub>O and brine, dried ( $\text{MgSO}_4$ ), filtered, and concentrated. Two additional separate reactions using **2k** (0.050 g, 0.34 mmol, and 0.150 g, 1.01 mmol) were carried out as described above. Crude product from the three reactions was combined and purified by silica gel flash chromatography (1% MeOH– $\text{CH}_2\text{Cl}_2$ ) to give **2j** (0.499 g, 79% combined yield) as a pale yellow solid. A small sample was further purified by recrystallization (EtOAc/hexanes) to give a white solid: mp (EtOAc/hexanes) 139–140 °C;  $^1\text{H-NMR}$  ( $\text{CDCl}_3$ )  $\delta$  7.46 (d, 1H,  $J = 8.7$  Hz), 6.95 (dd, 1H,  $J = 8.7$  Hz,  $J = 2.0$  Hz), 6.90 (d, 1H,  $J = 1.9$  Hz), 3.88 (t, 4H,  $J = 4.9$  Hz), 3.27 (t, 4H,  $J = 4.8$  Hz), 2.52 (s, 3H); EIMS  $m/e$  (rel intensity) 218 ( $\text{M}^+$ , 100); EIHRMS calcd for  $\text{C}_{12}\text{H}_{14}\text{N}_2\text{O}_2$  218.1056, found 218.1054.

**1,4-Piperidinedicarboxylic Acid, 1-(1,1-Dimethylethyl) Ester, 4-Ethyl Ester (3).** A solution of ethyl isonipecotate (20.0 g, 0.127 mol) and triethylamine (17.8 mL, 0.127 mol) in 1:1 dioxane–H<sub>2</sub>O (1.2 L) was cooled to 0 °C. After 15 min, di-*tert*-butyl dicarbonate (35.2 g, 0.161 mol) was added and the resulting mixture was allowed to warm to room temperature overnight. The mixture was extracted with EtOAc (4 $\times$ ),



and the combined organic layer was washed with 1 N HCl, H<sub>2</sub>O, and brine, dried (MgSO<sub>4</sub>), filtered, and concentrated to give a light orange oil. Kugelrohr distillation (0.05 Torr, 80–90 °C) gave **3** (30.69 g, 94%) as a colorless oil: <sup>1</sup>H-NMR (CDCl<sub>3</sub>) δ 4.11 (q, 2H, *J* = 7.2 Hz), 3.97–4.05 (m, 2H), 2.80 (br t, 2H, *J* = 11.6 Hz), 2.40 (tt, 1H, *J* = 11.0 Hz, *J* = 3.9 Hz), 1.81–1.86 (m, 2H), 1.52–1.66 (m, 2H), 1.43 (s, 9H), 1.23 (t, 3H, *J* = 7.2 Hz); EIMS *m/e* (rel intensity) 257 (M<sup>+</sup>, 32), 156 (100); EIHRMS calcd for C<sub>13</sub>H<sub>23</sub>NO<sub>4</sub> 257.1627, found 257.1601.

**4-(Hydroxymethyl)-1-piperidinecarboxylic Acid, 1-(1,1-Dimethylethyl) Ester (4).** Lithium aluminum hydride (4.3 g, 0.114 mol) was added to a cold solution (0 °C) of **3** (26.57 g, 0.103 mol) in THF (1 L). After 30 min, the ice bath was removed and the reaction mixture was allowed to stir overnight at room temperature. Sodium sulfate decahydrate was added carefully until evolution of gas subsided. After stirring for 1 h, the mixture was filtered through a Celite pad and the filtrate was concentrated. Recrystallization (Et<sub>2</sub>O/hexanes) gave **4** (20.67 g, 93%) as a white solid: mp (Et<sub>2</sub>O/hexanes) 80–81 °C; <sup>1</sup>H-NMR (CDCl<sub>3</sub>) δ 4.04–4.26 (m, 2H), 3.49 (d, 2H, *J* = 6.4 Hz), 2.70 (br t, 2H, *J* = 12.0 Hz), 1.60–1.73 (m, 3H), 1.47 (s, 9H), 1.15 (ddd, 2H, *J* = 23.2 Hz, *J* = 12.0 Hz, *J* = 4.3 Hz); CIMS *m/e* (rel intensity) 216 ([M + 1]<sup>+</sup>, 80), 160 (100). Anal. (C<sub>11</sub>H<sub>21</sub>NO<sub>3</sub>) C, H, N.

**4-(Iodomethyl)-1-piperidinecarboxylic Acid, 1-(1,1-Dimethylethyl) Ester (5).** Triphenylphosphine (31.0 g, 0.119 mol) was added to a mixture of iodine (29.0 g, 0.114 mol) in benzene (1 L). After 5 min, pyridine (18.5 mL, 0.228 mol) followed by alcohol **4** (20.5 g, 0.095 mol) was added. The resulting mixture was heated to reflux for 1.5 h. The cooled reaction mixture was filtered, and the filtrate was washed with saturated Na<sub>2</sub>S<sub>2</sub>O<sub>3</sub> and brine, dried (MgSO<sub>4</sub>), filtered, and concentrated. Purification by silica gel chromatography (10% → 20% EtOAc–hexanes) gave **5** (28.5 g, 92%) as a clear oil. Upon standing, a white solid was obtained. **5**: mp 58–59 °C; <sup>1</sup>H-NMR (CDCl<sub>3</sub>) δ 4.09 (br d, 2H, *J* = 13.1 Hz), 3.08 (d, 2H, *J* = 6.5 Hz), 2.66 (br t, 2H, *J* = 13.1 Hz), 1.80 (br d, 2H, *J* = 12.9 Hz), 1.52–1.64 (m, 1H), 1.43 (s, 9H), 1.11 (ddd, 2H, *J* = 24.7 Hz, *J* = 12.7 Hz, *J* = 4.3 Hz); FABMS *m/e* (rel intensity) 326 ([M + 1]<sup>+</sup>, 100). Anal. (C<sub>11</sub>H<sub>20</sub>INO<sub>2</sub>) C, H, N.

**4-[2-(1,2-Benzisoxazol-3-yl)ethyl]-1-piperidinecarboxylic Acids, 1-(1,1-Dimethylethyl) Esters 6a–f, m. Method A.** A mixture of **2a** (0.410 g, 3.08 mmol) and iodide **5** (1.05 g, 3.23 mmol) in dry THF (3.2 mL) was cooled to –78 °C. Freshly prepared 1 M LDA (3.1 mL, 3.1 mmol) was added dropwise, and the resulting yellow-orange solution was stirred for 25 min at –78 °C. Saturated NH<sub>4</sub>Cl was added, and the mixture was extracted with EtOAc (3×). The combined organic layer was washed with brine, dried (MgSO<sub>4</sub>), filtered, and concentrated. Purification by silica gel flash chromatography (10% → 20% EtOAc–hexanes) gave **6a** (0.430 g, 42%) as a colorless oil: <sup>1</sup>H-NMR (CDCl<sub>3</sub>) δ 7.62 (d, 1H, *J* = 8.0 Hz), 7.49–7.55 (m, 2H), 7.25–7.31 (m, 1H), 4.09 (m, 2H), 3.00 (t, 2H, *J* = 7.8 Hz), 2.66 (br t, 2H, *J* = 13.0 Hz), 1.71–1.84 (m, 4H), 1.47–1.53 (m, 1H), 1.43 (s, 9H), 1.14 (ddd, 2H, *J* = 24.5 Hz, *J* = 12.1 Hz, *J* = 4.1 Hz); FABMS *m/e* (rel intensity) 331 ([M + 1]<sup>+</sup>, 18), 231 (100); FABHRMS calcd for C<sub>19</sub>H<sub>27</sub>N<sub>2</sub>O<sub>3</sub> 331.2022, found 331.2021.

A similar procedure was followed for the preparation of **6b–f, m** starting from the corresponding 3-methyl-1,2-benzisoxazoles **2b–f, m**.

**6b**: 78%; oil; <sup>1</sup>H-NMR (CDCl<sub>3</sub>) δ 7.28–7.40 (m, 3H), 4.04–4.11 (m, 2H), 2.94 (t, 2H, *J* = 7.8 Hz), 2.64 (br t, 2H, *J* = 12.3 Hz), 2.43 (s, 3H), 1.70–1.99 (m, 4H), 1.42 (s, 9H), 1.41–1.55 (m, 1H), 1.13 (ddd, 2H, *J* = 24.4 Hz, *J* = 12.0 Hz, *J* = 4.1 Hz); EIMS *m/e* (rel intensity) 344 (M<sup>+</sup>, 10), 271 (100); EIHRMS calcd for C<sub>20</sub>H<sub>28</sub>N<sub>2</sub>O<sub>3</sub> 344.2099, found 344.2073.

**6c**: 78%; oil; <sup>1</sup>H-NMR (CDCl<sub>3</sub>) δ 7.32 (s, 1H), 7.27 (s, 1H), 4.04–4.10 (m, 2H), 2.93 (t, 2H, *J* = 7.8 Hz), 2.64 (br t, 2H, *J* = 11.9 Hz), 2.35 (s, 3H), 2.32 (s, 3H), 1.70–1.80 (m, 4H), 1.43 (s, 9H), 1.43–1.51 (m, 1H), 1.13 (ddd, 2H, *J* = 24.3 Hz, *J* = 12.3 Hz, *J* = 4.2 Hz); EIMS *m/e* (rel intensity) 358 (M<sup>+</sup>, 20), 285 (100); EIHRMS calcd for C<sub>21</sub>H<sub>30</sub>N<sub>2</sub>O<sub>3</sub> 358.2255, found 3458.2263.

**6d**: 87%; oil; <sup>1</sup>H-NMR (CDCl<sub>3</sub>) δ 7.46 (d, 1H, *J* = 9.1 Hz), 7.17 (dd, 1H, *J* = 9.1 Hz, *J* = 2.5 Hz), 6.96 (d, 1H, *J* = 2.4 Hz), 4.09–4.16 (m, 2H), 3.87 (s, 3H), 2.99 (t, 2H, *J* = 7.8 Hz), 2.69

(br t, 2H, *J* = 12.3 Hz), 1.74–1.85 (m, 4H), 1.46–1.64 (m, 1H), 1.46 (s, 9H), 1.17 (ddd, 2H, *J* = 22.3 Hz, *J* = 12.2 Hz, *J* = 4.2 Hz); EIMS *m/e* (rel intensity) 360 (M<sup>+</sup>, 5), 259 (100); EIHRMS calcd for C<sub>20</sub>H<sub>28</sub>N<sub>2</sub>O<sub>4</sub> 360.2050, found 360.2053.

**6e**: 80%; mp 95–96 °C; <sup>1</sup>H-NMR (CDCl<sub>3</sub>) δ 7.47 (d, 1H, *J* = 8.7 Hz), 6.99 (d, 1H, *J* = 2.1 Hz), 6.91 (dd, 1H, *J* = 8.6 Hz, *J* = 2.1 Hz), 4.08–4.11 (m, 2H), 3.89 (s, 3H), 2.97 (t, 2H, *J* = 7.8 Hz), 2.68 (br t, 2H, *J* = 12.7 Hz), 1.72–1.84 (m, 4H), 1.46–1.60 (m, 1H), 1.46 (s, 9H), 1.16 (ddd, 2H, *J* = 24.6 Hz, *J* = 12.3 Hz, *J* = 4.3 Hz); CIMS *m/e* (rel intensity) 361 ([M + 1]<sup>+</sup>, 80), 261 (100). Anal. (C<sub>20</sub>H<sub>28</sub>N<sub>2</sub>O<sub>4</sub>) C, H, N.

**6f**: 62%; oil; <sup>1</sup>H-NMR (CDCl<sub>3</sub>) δ 7.12–7.19 (m, 2H), 6.91 (dd, 1H, *J* = 6.5 Hz, *J* = 2.2 Hz), 3.98–4.07 (m, 2H), 3.98 (s, 3H), 2.95 (t, 2H, *J* = 7.8 Hz), 2.62 (br t, 2H, *J* = 12.2 Hz), 1.67–1.78 (m, 4H), 1.40–1.48 (m, 1H), 1.40 (s, 9H), 1.11 (ddd, 2H, *J* = 24.5 Hz, *J* = 12.5 Hz, *J* = 4.3 Hz); EIMS *m/e* (rel intensity) 360 (M<sup>+</sup>, 5), 259 (100); EIHRMS calcd for C<sub>20</sub>H<sub>28</sub>N<sub>2</sub>O<sub>4</sub> 360.2050, found 360.2048.

**6m**: 27%; mp (CH<sub>2</sub>Cl<sub>2</sub>/hexanes) 100–102 °C; <sup>1</sup>H-NMR (CDCl<sub>3</sub>) δ 7.77 (s, 1H), 7.52 (d, 1H, *J* = 7.2 Hz), 7.45 (d, 1H, *J* = 7.2 Hz), 4.11 (br d, 2H, *J* = 14.3 Hz), 3.02 (t, 2H, *J* = 7.2 Hz), 2.70 (dt, 2H, *J* = 12.9 Hz, *J* = 3.6 Hz), 1.70–1.85 (m, 4H), 1.49 (s, 9H), 1.45–1.55 (m, 1H), 1.09–1.29 (m, 2H); CIMS *m/e* (rel intensity) 409 ([M + 1]<sup>+</sup>, 100); EIHRMS calcd for C<sub>19</sub>H<sub>25</sub>BrN<sub>2</sub>O<sub>3</sub> 410.1029, found 410.1049.

**4-[2-(1,2-Benzisoxazol-3-yl)ethyl]-1-piperidinecarboxylic Acids, 1-(1,1-Dimethylethyl) Esters 6g–j. Method B.** Freshly prepared 1 M LDA (11.0 mL, 11.0 mmol) was added dropwise (fast) to a cold (–78 °C) solution of **2g** (1.0 g, 5.26 mol) in THF (50 mL). Immediately after addition was complete, a solution of iodide **5** (1.71 g, 5.26 mmol) in THF (8 mL) was added all at once. The resulting yellow-orange solution was stirred for 30 min at –78 °C. Saturated NH<sub>4</sub>Cl was added, and the mixture was extracted with EtOAc (3×). The combined organic layer was washed with brine, dried (MgSO<sub>4</sub>), filtered, and concentrated. Purification by silica gel flash chromatography (20% → 50% EtOAc–CH<sub>2</sub>Cl<sub>2</sub>) gave **6g** (1.56 g, 76%) as a white solid: mp 142–143 °C; <sup>1</sup>H-NMR (CDCl<sub>3</sub>) δ 8.76 (s, 1H), 8.05 (s, 1H), 7.48 (d, 1H, *J* = 8.5 Hz), 7.32 (dd, 1H, *J* = 8.6 Hz, *J* = 1.5 Hz), 4.06 (br d, 2H, *J* = 11.5 Hz), 2.94 (t, 2H, *J* = 7.8 Hz), 2.66 (br t, 2H, *J* = 11.8 Hz), 2.20 (s, 3H), 1.69–1.80 (m, 4H), 1.41–1.47 (m, 1H), 1.44 (s, 9H), 1.12 (ddd, 2H, *J* = 23.8 Hz, *J* = 12.0 Hz, *J* = 3.9 Hz); EIMS *m/e* (rel intensity) 387 (M<sup>+</sup>, 20), 286 (100). Anal. (C<sub>21</sub>H<sub>29</sub>N<sub>3</sub>O<sub>4</sub>) C, H, N.

A similar procedure was followed for the preparation of **6h–j** starting from the corresponding 3-methyl-1,2-benzisoxazoles **2h–j**.

**6h**: 87%; mp 177–178.5 °C; <sup>1</sup>H-NMR (CDCl<sub>3</sub>) δ 8.61 (s, 1H), 8.15 (s, 1H), 7.86 (d, 2H, *J* = 7.4 Hz), 7.39–7.53 (m, 5H), 4.03 (br d, 2H, *J* = 12.7 Hz), 2.92 (t, 2H, *J* = 8.0 Hz), 2.50–2.73 (m, 2H), 1.60–1.80 (m, 4H), 1.40–1.45 (m, 1H), 1.41 (s, 9H), 1.13 (ddd, 2H, *J* = 24.0 Hz, *J* = 12.2 Hz, *J* = 3.8 Hz); CIMS *m/e* (rel intensity) 450 ([M + 1]<sup>+</sup>, 20), 394 (100). Anal. (C<sub>26</sub>H<sub>31</sub>N<sub>3</sub>O<sub>4</sub>) C, H, N.

**6i**: 81%; mp 66–67 °C; <sup>1</sup>H-NMR (CDCl<sub>3</sub>) δ 7.85 (dd, 2H, *J* = 8.3 Hz, *J* = 1.6 Hz), 7.35–7.57 (m, 6H), 7.02 (dd, 1H, *J* = 8.5 Hz, *J* = 1.6 Hz), 4.11 (br d, 2H, *J* = 13.2 Hz), 2.94 (t, 2H, *J* = 7.4 Hz), 2.68 (br t, 2H, *J* = 12.8 Hz), 1.71–1.77 (m, 4H), 1.46 (s, 9H), 1.46–1.55 (m, 1H), 1.15 (ddd, 2H, *J* = 23.6 Hz, *J* = 11.7 Hz, *J* = 3.9 Hz); EIMS *m/e* (rel intensity) 485 (M<sup>+</sup>, 50), 384 (100). Anal. (C<sub>25</sub>H<sub>31</sub>N<sub>3</sub>O<sub>5</sub>S) C, H, N.

**6j**: 62%; mp 164–165 °C; <sup>1</sup>H-NMR (CDCl<sub>3</sub>) δ 7.46 (d, 1H, *J* = 8.6 Hz), 6.92–6.97 (m, 2H), 4.02–4.15 (m, 2H), 3.89 (t, 4H, *J* = 4.9 Hz), 3.27 (t, 4H, *J* = 4.9 Hz), 2.95 (t, 2H, *J* = 7.8 Hz), 2.7 (br t, 2H, *J* = 12.1 Hz), 1.74–1.80 (m, 4H), 1.46–1.56 (m, 1H), 1.46 (s, 9H), 1.10–1.22 (m, 2H); EIMS *m/e* (rel intensity) 415 (M<sup>+</sup>, 15), 57 (100). Anal. (C<sub>23</sub>H<sub>33</sub>N<sub>3</sub>O<sub>4</sub>) C, H, N.

**3-[2-[1-(Phenylmethyl)-4-piperidinyl]ethyl]-1,2-benzisoxazoles 1a–h, j. Method C.** Trifluoroacetic acid (7 mL) was added dropwise to a cold (0 °C) solution of **6a** (0.50 g, 1.51 mmol) in CH<sub>2</sub>Cl<sub>2</sub> (7 mL). The resulting solution was stirred at 0 °C for 30 min. Volatiles were removed under reduced pressure, and excess trifluoroacetic acid was removed by concentrating from toluene twice. The crude product obtained was dissolved in CH<sub>2</sub>Cl<sub>2</sub> (10 mL), and triethylamine (0.42 mL,

3.01 mmol) followed by benzyl bromide (0.18 mL, 1.51 mmol) was added. The resulting mixture was stirred overnight (15 h) at room temperature. The mixture was washed with H<sub>2</sub>O and brine, dried (MgSO<sub>4</sub>), filtered, and concentrated. Purification by silica gel flash chromatography (50% EtOAc–hexanes) gave **1a**, free base (0.350 g, 73%) as a colorless oil. The maleate salt was prepared by adding a solution of maleic acid (0.108 g, 0.930 mmol) in Et<sub>2</sub>O (20 mL) to a solution of the free base (0.297 g, 0.926 mmol) in Et<sub>2</sub>O (20 mL). The white solid formed was collected and rinsed with Et<sub>2</sub>O to give **1a** (0.35 g, 87%) as the maleate salt: mp 146–148 °C; <sup>1</sup>H-NMR (CDCl<sub>3</sub>) δ 7.60 (d, 1H, *J* = 8.0 Hz), 7.51–7.52 (m, 2H), 7.37–7.49 (m, 5H), 7.27–7.32 (m, 1H), 6.30 (s, 2H), 4.16 (s, 2H), 3.45–3.51 (m, 2H), 2.98 (t, 2H, *J* = 7.4 Hz), 2.60–2.70 (m, 2H), 1.84–1.95 (m, 4H), 1.60–1.82 (m, 3H); CIMS *m/e* (rel intensity) 321 ([M + 1]<sup>+</sup>, 100). Anal. (C<sub>21</sub>H<sub>24</sub>N<sub>2</sub>O·C<sub>4</sub>H<sub>4</sub>O<sub>4</sub>) C, H, N.

A similar procedure was followed for the preparation of **1b–1h** starting from the corresponding benzisoxazoles **6b–6h**. In the cases of fumarate salt formation, fumaric acid (1 equiv) was dissolved in the minimum amount of EtOH before addition to a solution of the free base in Et<sub>2</sub>O or CH<sub>2</sub>Cl<sub>2</sub>.

**1b (maleate salt)**: 59%; mp 149–151 °C; <sup>1</sup>H-NMR (CDCl<sub>3</sub>) δ 7.27–7.43 (m, 8H), 6.32 (s, 2H), 4.17 (s, 2H), 3.51 (br d, 2H, *J* = 11.6 Hz), 2.96 (t, 2H, *J* = 7.3 Hz), 2.66 (br t, 2H, *J* = 10.8 Hz), 2.45 (s, 3H), 1.60–1.97 (m, 7H); CIMS *m/e* (rel intensity) 335 ([M + 1]<sup>+</sup>, 100). Anal. (C<sub>22</sub>H<sub>26</sub>N<sub>2</sub>O·C<sub>4</sub>H<sub>4</sub>O<sub>4</sub>) C, H, N.

**1c (maleate salt)**: 48%; mp 182–184 °C; <sup>1</sup>H-NMR (CDCl<sub>3</sub>) δ 7.30–7.41 (m, 7H), 6.32 (s, 2H), 4.17 (s, 2H), 3.51 (br d, 2H, *J* = 11.8 Hz), 2.95 (t, 2H, *J* = 7.2 Hz), 2.65 (br t, 2H, *J* = 11.7 Hz), 2.38 (s, 3H), 2.34 (s, 3H), 1.59–1.96 (m, 7H); CIMS *m/e* (rel intensity) 349 ([M + 1]<sup>+</sup>, 100). Anal. (C<sub>23</sub>H<sub>26</sub>N<sub>2</sub>O·C<sub>4</sub>H<sub>4</sub>O<sub>4</sub>·0.25H<sub>2</sub>O) C, H, N.

**1d (maleate salt)**: 44%; mp 144–145 °C; <sup>1</sup>H-NMR (CDCl<sub>3</sub>) δ 7.35–7.42 (m, 6H), 7.13 (dd, 1H, *J* = 9.1 Hz, *J* = 2.5 Hz), 6.92 (d, 1H, *J* = 2.4 Hz), 6.30 (s, 2H), 4.17 (s, 2H), 3.83 (s, 3H), 3.46–3.51 (m, 2H), 2.94 (t, 2H, *J* = 7.3 Hz), 2.60–2.80 (m, 2H), 1.60–1.96 (m, 7H); CIMS *m/e* (rel intensity) 351 ([M + 1]<sup>+</sup>, 100). Anal. (C<sub>22</sub>H<sub>26</sub>N<sub>2</sub>O<sub>2</sub>·C<sub>4</sub>H<sub>4</sub>O<sub>4</sub>) C, H, N.

**1e (free base)**: 55%; mp (Et<sub>2</sub>O/hexanes) 91–92 °C; <sup>1</sup>H-NMR (CDCl<sub>3</sub>) δ 7.47 (d, 1H, *J* = 8.7 Hz), 7.21–7.33 (m, 5H), 6.98 (d, 1H, *J* = 1.8 Hz), 6.90 (dd, 1H, *J* = 8.7 Hz, *J* = 2.0 Hz), 3.88 (s, 3H), 3.50 (s, 2H), 2.88–2.98 (m, 4H), 1.96 (br t, 2H, *J* = 10.6 Hz), 1.74–1.83 (m, 4H), 1.27–1.34 (m, 3H); CIMS *m/e* (rel intensity) 351 ([M + 1]<sup>+</sup>, 100). Anal. (C<sub>22</sub>H<sub>26</sub>N<sub>2</sub>O<sub>2</sub>) C, H, N.

**1f (fumarate salt)**: 14%; mp 138–139 °C; <sup>1</sup>H-NMR (CDCl<sub>3</sub>) δ 7.27–7.41 (m, 7H), 7.19 (d, 1H, *J* = 7.7 Hz), 6.59 (s, 2H), 3.97 (s, 3H), 3.65 (s, 2H), 2.90–3.01 (m, 4H), 2.18 (br t, 2H, *J* = 10.8 Hz), 1.67–1.77 (m, 4H), 1.26–1.32 (m, 3H); EIMS *m/e* (rel intensity) 350 (M<sup>+</sup>, 10), 333 (100). Anal. (C<sub>22</sub>H<sub>26</sub>N<sub>2</sub>O<sub>2</sub>·C<sub>4</sub>H<sub>4</sub>O<sub>4</sub>) C, H, N.

**1g (fumarate salt)**: 42%; mp (EtOH) 225–226 °C; <sup>1</sup>H-NMR (DMSO-*d*<sub>6</sub>) δ 10.37 (s, 1H), 8.13 (s, 1H), 7.76 (d, 1H, *J* = 8.5 Hz), 7.25–7.36 (m, 6H), 6.59 (s, 1H), 3.54 (s, 2H), 2.83–2.96 (m, 4H), 2.10 (s, 3H), 2.01 (br t, 2H, *J* = 11.1 Hz), 1.69–1.73 (m, 4H), 1.20–1.28 (m, 3H); CIMS *m/e* (rel intensity) 378 ([M + 1]<sup>+</sup>, 100). Anal. (C<sub>23</sub>H<sub>27</sub>N<sub>3</sub>O<sub>2</sub>·0.5C<sub>4</sub>H<sub>4</sub>O<sub>4</sub>·0.25H<sub>2</sub>O) C, H, N.

**1h (maleate salt)**: 26%; mp 182–183 °C; <sup>1</sup>H-NMR (DMSO-*d*<sub>6</sub>) δ 10.65 (s, 1H), 8.31 (s, 1H), 7.98 (d, 2H, *J* = 7.2 Hz), 7.85 (d, 1H, *J* = 8.6 Hz), 7.48–7.71 (m, 9H), 6.03 (s, 2H), 4.25 (br s, 2H), 3.20–3.60 (m, 4H), 2.89–3.02 (m, 4H), 1.40–1.97 (m, 5H); EIMS *m/e* (rel intensity) 439 (M<sup>+</sup>, 10), 422 (100). Anal. (C<sub>23</sub>H<sub>29</sub>N<sub>3</sub>O<sub>2</sub>·C<sub>4</sub>H<sub>4</sub>O<sub>4</sub>) C, H, N.

**1j (free base)**: 75%; mp (EtOH) 129–130 °C; <sup>1</sup>H-NMR (CDCl<sub>3</sub>) δ 7.44 (d, 1H, *J* = 8.7 Hz), 7.23–7.30 (m, 5H), 6.89–6.93 (m, 2H), 3.87 (t, 4H, *J* = 4.8 Hz), 3.47 (s, 2H), 3.25 (t, 4H, *J* = 4.8 Hz), 2.85–2.94 (m, 4H), 1.92 (br t, 2H, *J* = 10.8 Hz), 1.72–1.79 (m, 4H), 1.21–1.31 (m, 3H); CIMS *m/e* (rel intensity) 406 ([M + 1]<sup>+</sup>, 100). Anal. (C<sub>25</sub>H<sub>31</sub>N<sub>3</sub>O<sub>2</sub>) C, H, N.

**6-Benzenesulfonamido-3-[2-[1-(phenylmethyl)-4-piperidinyl]ethyl]-1,2-benzisoxazole, Fumarate Salt (1i)**. Trimethylsilyl trifluoromethanesulfonate (1.30 mL, 6.76 mmol) was added dropwise to a cold (0 °C) solution of **6i** (0.819 g, 1.69 mmol) and 2,6-lutidine (0.590 mL, 5.07 mmol) in CH<sub>2</sub>Cl<sub>2</sub> (17 mL). After 1.5 h, saturated NaHCO<sub>3</sub> was added and the resulting mixture was stirred at room temperature for 15 min. The white precipitate formed was collected by filtration and

redissolved in H<sub>2</sub>O at pH 2. This acidic aqueous layer was extracted with CH<sub>2</sub>Cl<sub>2</sub> (2×) and EtOAc (1×). All organic layers were combined, dried (MgSO<sub>4</sub>), filtered, and concentrated. The crude white solid obtained was suspended in 3:5 THF–DMF (80 mL), and triethylamine (0.40 mL, 2.86 mmol) followed by benzyl bromide (0.22 mL, 1.86 mmol) was added. The resulting mixture was stirred at room temperature for 24 h. The reaction mixture was concentrated, and CH<sub>2</sub>Cl<sub>2</sub> was added to the residue. The organic layer was washed with H<sub>2</sub>O and brine, dried (MgSO<sub>4</sub>), filtered, and concentrated. Purification by silica gel flash chromatography (CH<sub>2</sub>Cl<sub>2</sub> → 5% MeOH–CH<sub>2</sub>Cl<sub>2</sub>) gave **1i**, free base (0.334 g, 49%) as a white foam. The fumarate salt was prepared by adding a solution of fumaric acid (0.040 g, 0.345 mmol) in EtOH (3 mL) to a solution of the free base (0.150 g, 0.315 mmol) in CH<sub>2</sub>Cl<sub>2</sub> (6 mL). After concentrating, the residue was triturated with Et<sub>2</sub>O to give **1i**, fumarate salt (0.151 g, 81%) as a white solid: mp >100 °C dec; <sup>1</sup>H-NMR (DMSO-*d*<sub>6</sub>) δ 7.82 (d, 2H, *J* = 7.0 Hz), 7.70 (d, 1H, *J* = 8.6 Hz), 7.51–7.60 (m, 3H), 7.27–7.32 (m, 6H), 7.07 (dd, 1H, *J* = 8.6 Hz, *J* = 1.6 Hz), 6.59 (s, 2H), 3.55 (s, 2H), 2.82–2.90 (m, 4H), 2.03 (br t, 2H, *J* = 11.5 Hz), 1.61–1.70 (m, 4H), 1.20–1.25 (m, 3H); CIMS *m/e* (rel intensity) 476 ([M + 1]<sup>+</sup>, 100). Anal. (C<sub>27</sub>H<sub>29</sub>N<sub>3</sub>O<sub>3</sub>·S·C<sub>4</sub>H<sub>4</sub>O<sub>4</sub>·0.5H<sub>2</sub>O) C, H, N.

**6-Bromo-3-[2-[1-(phenylmethyl)-4-piperidinyl]ethyl]-1,2-benzisoxazole, Maleate Salt (1m)**. Trifluoroacetic acid (1.25 mL) was added dropwise to a cold (0 °C) solution of **6m** (0.43 g, 1.05 mmol) in CH<sub>2</sub>Cl<sub>2</sub> (5 mL). The resulting solution was stirred at 0 °C for 30 min. Volatiles were removed under reduced pressure, and excess trifluoroacetic acid was removed by concentrating from toluene twice. The crude product obtained was dissolved in DMF (10 mL), and Na<sub>2</sub>CO<sub>3</sub> (0.56 g, 5.23 mmol) followed by benzyl bromide (0.16 mL, 1.36 mmol) was added. The resulting mixture was stirred at room temperature for 2 h. The reaction mixture was filtered and concentrated under reduced pressure. The residue was partitioned between EtOAc and saturated NaHCO<sub>3</sub>. The separated organic layer was washed with brine, dried (MgSO<sub>4</sub>), filtered, and concentrated. Purification by silica gel flash chromatography (5% MeOH–CH<sub>2</sub>Cl<sub>2</sub>) gave **1m**, free base (0.279 g, 67%) as a pale yellow oil. The maleate salt was prepared by adding a solution of maleic acid (0.021 g, 0.196 mmol) in EtOH (1 mL) to a solution of the free base (0.071 g, 0.178 mmol) in CH<sub>2</sub>Cl<sub>2</sub> (2 mL). After concentrating, **1m**, maleate salt (0.55 g, 60%) was obtained as a white solid: mp (EtOH) 157–158 °C; <sup>1</sup>H-NMR (DMSO-*d*<sub>6</sub>) δ 8.08 (s, 1H), 7.87 (d, 1H, *J* = 8.4 Hz), 7.58 (d, 1H, *J* = 8.5 Hz), 7.47 (s, 5H), 6.03 (s, 2H), 4.23 (br s, 2H), 3.25–3.40 (m, 2H), 3.02 (t, 2H, *J* = 7.5 Hz), 2.80–2.95 (m, 2H), 1.88–2.00 (m, 2H), 1.70–1.80 (m, 2H), 1.30–1.60 (m, 3H); EIMS *m/e* (rel intensity) 399 (M<sup>+</sup>, 10), 185 (100); EIHRMS calcd for C<sub>21</sub>H<sub>23</sub>BrN<sub>2</sub>O 398.0994, found 398.0926. Anal. (C<sub>21</sub>H<sub>23</sub>BrN<sub>2</sub>O·0.75C<sub>4</sub>H<sub>4</sub>O<sub>4</sub>) C, H, N.

**6-Hydroxy-3-[2-[1-(phenylmethyl)-4-piperidinyl]ethyl]-1,2-benzisoxazole (1l)**. A mixture of **1e** (0.11 g, 0.288 mmol) in 48% aqueous HBr (10 mL) was heated at 110 °C for 16 h. The mixture was made basic by addition of saturated NaHCO<sub>3</sub> and extracted with CH<sub>2</sub>Cl<sub>2</sub>. The organic layer was dried (MgSO<sub>4</sub>), filtered, and concentrated. Purification by silica gel flash chromatography (3% → 6% MeOH–CH<sub>2</sub>Cl<sub>2</sub>) gave **1l** (0.055 g, 57%) as a white solid: mp 148–149 °C; <sup>1</sup>H-NMR (CDCl<sub>3</sub>) δ 7.70 (br s, 1H), 7.27–7.37 (m, 6H), 6.74–6.80 (m, 2H), 3.63 (s, 2H), 3.04 (br d, 2H, *J* = 10.8 Hz), 2.88 (t, 2H, *J* = 7.7 Hz), 2.05–2.20 (m, 2H), 1.65–1.95 (m, 4H), 1.30–1.60 (m, 3H); EIMS *m/e* (rel intensity) 336 (M<sup>+</sup>, 20), 91 (100); EIHRMS calcd for C<sub>21</sub>H<sub>24</sub>N<sub>2</sub>O<sub>2</sub> 336.1838, found 336.1819.

**6-Amino-3-[2-[1-(phenylmethyl)-4-piperidinyl]ethyl]-1,2-benzisoxazole, Maleate Salt (1k)**. A mixture of **1g** (0.30 g, 0.79 mmol) in 1 N HCl (10 mL) was heated to reflux for 30 min. The cooled reaction mixture was made basic with 10% NaOH and extracted with EtOAc (2×). The combined organic layer was washed with brine, dried (MgSO<sub>4</sub>), filtered, and concentrated to give **1k**, free base (0.259 g, 98%) as an oil. The monomaleate salt was prepared by adding a solution of maleic acid (0.099 g, 0.85 mmol) in EtOH (3 mL) to a solution of the free base (0.259 g, 0.77 mmol) in CH<sub>2</sub>Cl<sub>2</sub>. After concentrating, the residue was triturated with Et<sub>2</sub>O to give **1k**, maleate salt (0.29 g, 64%) as a white powder: mp 173–174 °C; <sup>1</sup>H-NMR

(DMSO-*d*<sub>6</sub>) δ 7.41–7.47 (m, 6H), 6.58–6.63 (m, 2H), 6.06 (s, 2H), 5.87 (br s, 2H), 4.26 (s, 2H), 3.29–3.38 (m, 2H), 2.80–2.95 (m, 4H), 1.90 (br d, 2H, *J* = 12.5 Hz), 1.25–1.80 (m, 5H); CIMS *m/e* (rel intensity) 336 ([M + 1]<sup>+</sup>, 100). Anal. (C<sub>21</sub>H<sub>25</sub>N<sub>3</sub>O·C<sub>4</sub>H<sub>4</sub>O<sub>4</sub>) C, H, N.

**6-Cyano-3-[2-[1-(phenylmethyl)-4-piperidinyl]ethyl]-1,2-benzisoxazole (1n).** A solution of NaNO<sub>2</sub> (0.112 g, 1.62 mmol) in H<sub>2</sub>O (4 mL) was added to a solution of **1k** (0.534 g, 1.59 mmol) in 28% HCl (20 mL) kept at 0 °C. The resulting mixture was neutralized to pH 7 by cautious addition of solid Na<sub>2</sub>CO<sub>3</sub>. The neutral mixture was added in portions to a well-stirred mixture of toluene (75 mL), ice, and a freshly prepared solution of CuCN (*Organic Syntheses*; Collect. Vol. I, p 514; CuSO<sub>4</sub>: 0.318 g, 1.99 mmol). The mixture obtained was kept at 0 °C for 30 min and then at room temperature for 2 h and, finally, heated at 50 °C for 5 min. The mixture was extracted with ethyl acetate, and the organic phase was washed with H<sub>2</sub>O and brine, dried (MgSO<sub>4</sub>), filtered, and concentrated. Purification by silica gel flash chromatography (3% MeOH–CH<sub>2</sub>Cl<sub>2</sub>) gave **1n** (0.236 g, 43%) as a pale orange solid. Recrystallization (EtOH/hexanes) of a small sample gave **1n** as an off-white solid: mp (EtOH/hexanes) 113–114.5 °C; <sup>1</sup>H-NMR (CDCl<sub>3</sub>) δ 7.89 (s, 1H), 7.77 (d, 1H, *J* = 8.4 Hz), 7.57 (d, 1H, *J* = 8.7 Hz), 7.24–7.33 (m, 5H), 3.51 (s, 2H), 3.04 (t, 2H, *J* = 7.9 Hz), 2.92 (br d, 2H, *J* = 11.2 Hz), 1.97 (br t, 2H, *J* = 10.7 Hz), 1.74–1.85 (m, 4H), 1.26–1.40 (m, 3H); FABMS *m/e* (rel intensity) 346 ([M + 1]<sup>+</sup>, 20), 119 (100). Anal. (C<sub>22</sub>H<sub>23</sub>N<sub>3</sub>O) C, H, N.

**6-Carbamoyl-3-[2-[1-(phenylmethyl)-4-piperidinyl]ethyl]-1,2-benzisoxazole (1o).** Powdered KOH (0.150 g, 2.68 mmol) was added to a mixture of **1n** (0.250 g, 0.724 mmol) in *t*-BuOH (10 mL). The resulting mixture was heated at 85 °C for 20 min. The cooled reaction mixture was poured over brine and extracted with CH<sub>2</sub>Cl<sub>2</sub>. The organic phase was washed with 10% NaOH and brine, dried (MgSO<sub>4</sub>), filtered, and concentrated. The crude product was purified by recrystallization (EtOAc/hexanes) to give **1o** (0.114 g, 43%) as a white solid: mp (EtOAc/hexanes) 181–182 °C; <sup>1</sup>H-NMR (DMSO-*d*<sub>6</sub>) δ 8.20 (br s, 1H), 8.15 (s, 1H), 7.97 (d, 1H, *J* = 8.4 Hz), 7.87 (d, 1H, *J* = 8.1 Hz), 7.64 (br s, 1H), 7.22–7.31 (m, 5H), 3.42 (s, 2H), 3.02 (t, 2H, *J* = 7.8 Hz), 2.78 (br d, 2H, *J* = 11.5 Hz), 1.87 (br t, 2H, *J* = 10.9 Hz), 1.69–1.73 (m, 4H), 1.22–1.26 (m, 3H); EIMS *m/e* (rel intensity) 363 (M<sup>+</sup>, 2), 91 (100). Anal. (C<sub>22</sub>H<sub>25</sub>N<sub>3</sub>O<sub>2</sub>) C, H, N.

**4-(Iodoethyl)-1-piperidinecarboxylic Acid, 1-(1,1-Dimethylethyl) Ester (13).** The procedure described for the preparation of iodide **5** was followed with **12**<sup>53</sup> (1.74 g, 7.59 mmol), triphenylphosphine (2.49 g, 9.49 mmol), iodine (2.31 g, 9.11 mmol), and pyridine (1.5 mL, 18.2 mmol) in benzene (50 mL) to give **13** (2.27 g, 98%) as a colorless oil: <sup>1</sup>H-NMR (CDCl<sub>3</sub>) δ 4.09 (br d, 2H, *J* = 11.4 Hz), 3.22 (t, 2H, *J* = 7.3 Hz), 2.20 (br t, 2H, *J* = 12.5 Hz), 1.78 (q, 2H, *J* = 6.9 Hz), 1.47–1.68 (m, 3H), 1.46 (s, 9H), 1.12 (ddd, 2H, *J* = 24.3 Hz, *J* = 12 Hz, *J* = 4.3 Hz); EIMS *m/e* (rel intensity) 339 (M<sup>+</sup>, 62), 156 (100); EIHRMS calcd for C<sub>12</sub>H<sub>22</sub>INO<sub>2</sub> 339.0696, found 339.0705.

**4-[3-(1,2-Benzisoxazol-3-yl)propyl]-1-piperidinecarboxylic Acid, 1-(1,1-Dimethylethyl) Ester (14).** Method A was followed with **2a** (0.412 g, 3.09 mmol), iodide **13** (1.15 g, 3.4 mmol), and 1 M LDA (3.4 mL, 3.4 mmol) in THF (8 mL) to give **14** (0.694 g, 65%) as a pale yellow oil: <sup>1</sup>H-NMR (CDCl<sub>3</sub>) δ 7.65 (d, 1H, *J* = 8.0 Hz), 7.54–7.57 (m, 2H), 7.27–7.34 (m, 1H), 4.08 (br d, 2H, *J* = 12.5 Hz), 2.99 (t, 2H, *J* = 7.6 Hz), 2.66 (br t, 2H, *J* = 12.0 Hz), 1.86–1.92 (m, 2H), 1.63–1.68 (m, 4H), 1.45 (s, 9H), 1.36–1.45 (m, 1H), 1.06–1.12 (m, 2H); EIMS *m/e* (rel intensity) 344 (M<sup>+</sup>, 5), 243 (100); EIHRMS calcd for C<sub>20</sub>H<sub>28</sub>N<sub>2</sub>O<sub>3</sub> 344.2100, found 344.2102.

**3-[3-[1-(Phenylmethyl)-4-piperidinyl]propyl]-1,2-benzisoxazole, Maleate Salt (7).** Method C was followed with **14** (0.544 g, 1.58 mmol) and trifluoroacetic acid (4 mL) in CH<sub>2</sub>Cl<sub>2</sub> (16 mL) followed by triethylamine (1.1 mL, 7.9 mmol) and benzyl bromide (0.21 mL, 1.74 mmol) in CH<sub>2</sub>Cl<sub>2</sub> (10 mL) for 7.25 h. Purification by chromatography (2% → 5% MeOH–CH<sub>2</sub>Cl<sub>2</sub>) gave **7**, free base (0.285 g, 54%) as a pale yellow oil. The maleate salt was prepared by adding maleic acid (0.109 g, 0.94 mmol) dissolved in the minimum amount of EtOH to a

solution of the free base (0.285 g, 0.85 mmol) in CH<sub>2</sub>Cl<sub>2</sub> (10 mL). After concentrating, the residue was purified by recrystallization (EtOAc) to give **7**, maleate salt (0.292 g, 76%) as an off-white solid: mp (EtOAc) 134.5–135.5 °C; <sup>1</sup>H-NMR (DMSO-*d*<sub>6</sub>) δ 7.90 (d, 1H, *J* = 7.9 Hz), 7.61–7.72 (m, 2H), 7.47 (s, 5H), 7.38 (t, 1H, *J* = 7.3 Hz), 6.04 (s, 2H), 4.26 (br s, 2H), 3.22–3.45 (m, 2H), 2.99 (t, 2H, *J* = 7.4 Hz), 2.70–2.96 (m, 2H), 1.70–1.90 (m, 4H), 1.40–1.65 (m, 1H), 1.20–1.40 (m, 4H); EIMS *m/e* (rel intensity) 334 (M<sup>+</sup>, 20), 173 (100). Anal. (C<sub>22</sub>H<sub>26</sub>N<sub>2</sub>O·C<sub>4</sub>H<sub>4</sub>O<sub>4</sub>) C, H, N.

**(E)-3-[2-[1-(Phenylmethyl)-4-piperidinyl]ethenyl]-1,2-benzisoxazole, Maleate Salt (8).** NaH (60% mineral oil dispersion, 0.10 g, 2.51 mmol) was added to a mixture of 3-(triphenylphosphoniummethyl)-1,2-benzisoxazole bromide (**15**)<sup>21</sup> (1.19 g, 2.51 mmol) in THF (10 mL). After the mixture had stirred at room temperature for 1 h, a solution of aldehyde **16**<sup>54</sup> (0.51 g, 2.51 mmol) in THF (2 mL) was added. The mixture obtained was stirred for 4 h and filtered. The filtrate was concentrated, and the residue was partitioned between Et<sub>2</sub>O and H<sub>2</sub>O. The separated organic layer was dried (MgSO<sub>4</sub>), filtered, and concentrated. Purification by silica gel flash chromatography (40% EtOAc–hexanes) gave **8**, free base (0.483 g, 60%) as a colorless oil. The maleate salt was prepared by adding maleic acid (0.194 g, 1.67 mmol) dissolved in the minimum amount of EtOH to a solution of the free base (0.483 g, 1.52 mmol) in Et<sub>2</sub>O (25 mL). The white solid obtained was collected by filtration to give **8**, maleate salt (0.581 g, 88%): mp 174–175 °C; <sup>1</sup>H-NMR (DMSO-*d*<sub>6</sub>) δ 8.16 (d, 1H, *J* = 7.8 Hz), 7.75 (d, 1H, *J* = 8.4 Hz), 7.67 (t, 1H, *J* = 8.2 Hz), 7.41–7.55 (m, 6H), 6.96 (br dd, 1H, *J* = 16.5 Hz, *J* = 5.6 Hz), 6.78 (d, 1H, *J* = 16.5 Hz), 6.08 (s, 2H), 4.33 (s, 2H), 3.32–3.39 (m, 2H), 2.95–3.15 (m, 2H), 2.50–2.70 (m, 1H), 2.06 (br d, 2H, *J* = 12.6 Hz), 1.60–1.90 (m, 2H); EIMS *m/e* (rel intensity) 318 (M<sup>+</sup>, 20), 91 (100). Anal. (C<sub>21</sub>H<sub>22</sub>N<sub>2</sub>O·C<sub>4</sub>H<sub>4</sub>O<sub>4</sub>) C, H, N.

**4-[[1,2-Benzisoxazol-3-yl]oxy]methyl]-1-piperidinecarboxylic Acid, 1-(1,1-Dimethylethyl) Ester (17).** NaH (60% mineral oil dispersion, 0.941 g, 23.53 mmol) was added in portions to a solution of alcohol **4** (4.82 g, 22.41 mmol) in DMF (220 mL) at 0 °C. After 10 min, the reaction mixture was warmed to room temperature and 3-chloro-1,2-benzisoxazole<sup>22</sup> (3.44 g, 22.41 mmol) was added. The mixture obtained was heated at 115 °C for 16 h. The reaction mixture was diluted with EtOAc, washed with H<sub>2</sub>O (4×) and brine, dried (MgSO<sub>4</sub>), filtered, and concentrated. Purification by silica gel flash chromatography (10% EtOAc–hexanes) gave **17** (4.16 g, 56%) as a white solid: mp 103–104.5 °C; <sup>1</sup>H-NMR (CDCl<sub>3</sub>) δ 7.61 (d, 1H, *J* = 7.9 Hz), 7.48–7.54 (m, 1H), 7.41 (d, 1H, *J* = 8.5 Hz), 7.22–7.27 (m, 1H), 4.28 (d, 2H, *J* = 6.5 Hz), 4.16 (br d, 2H, *J* = 13.3 Hz), 2.75 (dt, 2H, *J* = 13.2 Hz, *J* = 2.6 Hz), 2.04–2.13 (m, 1H), 1.83 (br d, 2H, *J* = 13.7 Hz), 1.45 (s, 9H), 1.30 (ddd, 2H, *J* = 24.9 Hz, *J* = 12.5 Hz, *J* = 4.2 Hz); CIMS *m/e* (rel intensity) 333 ([M + 1]<sup>+</sup>, 100). Anal. (C<sub>18</sub>H<sub>24</sub>N<sub>2</sub>O<sub>4</sub>) C, H, N.

**3-[[1-(Phenylmethyl)-4-piperidinyl]methoxy]-1,2-benzisoxazole, Fumarate Salt (9).** Method C was followed with **17** (0.827 g, 2.49 mmol) and trifluoroacetic acid (10 mL) in CH<sub>2</sub>Cl<sub>2</sub> (25 mL) followed by triethylamine (0.58 mL, 4.13 mmol) and benzyl bromide (0.128 mL, 1.07 mmol) in CH<sub>2</sub>Cl<sub>2</sub> (8 mL) overnight (18 h). Purification by chromatography (5% MeOH–CH<sub>2</sub>Cl<sub>2</sub>) gave **9**, free base (0.199 g, 75%) as an off-white solid. The fumarate salt was prepared by adding fumaric acid (0.074 g, 0.633 mmol) dissolved in the minimum amount of EtOH to a solution of the free base (0.186 g, 0.58 mmol) in CH<sub>2</sub>Cl<sub>2</sub> (6 mL). After concentrating, the residue was purified by recrystallization (EtOH/Et<sub>2</sub>O) to give **9**, fumarate salt (0.134 g, 53%) as an off-white solid: mp (EtOH/Et<sub>2</sub>O) 163–164 °C; <sup>1</sup>H-NMR (DMSO-*d*<sub>6</sub>) δ 7.74 (d, 1H, *J* = 7.8 Hz), 7.61–7.69 (m, 2H), 7.26–7.41 (m, 6H), 6.60 (s, 2H), 4.28 (d, 2H, *J* = 6.4 Hz), 3.65 (s, 2H), 2.97 (br d, 2H, *J* = 11.4 Hz), 2.20 (br t, 2H, *J* = 11.7 Hz), 1.90–2.05 (m, 1H), 1.81 (br d, 2H, *J* = 12.8 Hz), 1.38–1.49 (m, 2H); EIMS *m/e* (rel intensity) 322 (M<sup>+</sup>, 30), 91 (100). Anal. (C<sub>20</sub>H<sub>22</sub>N<sub>2</sub>O<sub>2</sub>·C<sub>4</sub>H<sub>4</sub>O<sub>4</sub>·0.75H<sub>2</sub>O) C, H, N.

**3-[[[1-(Phenylmethyl)-4-piperidinyl]methyl]amino]-1,2-benzisoxazole (10).** A mixture of 3-chloro-1,2-benzisoxazole<sup>22</sup> (0.238 g, 1.55 mmol), 4-(aminomethyl)-1-(phenylmethyl)-piperidine (**18**)<sup>23</sup> (0.316 g, 1.55 mmol), and K<sub>2</sub>CO<sub>3</sub> (0.214 g, 1.55

mmol) in DMSO (10 mL) was heated at 150 °C for 20 h. The cooled reaction mixture was diluted with EtOAc (75 mL) and poured over H<sub>2</sub>O (200 mL). The organic phase was separated, washed with brine, dried (MgSO<sub>4</sub>), filtered, and concentrated. The brown oil obtained was purified by silica gel flash chromatography (4% MeOH-CH<sub>2</sub>Cl<sub>2</sub>) to give **10** (0.084 g, 17%) as a pale yellow oil: <sup>1</sup>H-NMR (CDCl<sub>3</sub>) δ 7.44–7.50 (m, 2H), 7.38 (d, 1H, *J* = 8.8 Hz), 7.16–7.31 (m, 6H), 4.35–4.42 (m, 1H), 3.51 (s, 2H), 3.33 (t, 2H, *J* = 6.2 Hz), 2.92 (br d, 2H, *J* = 11.5 Hz), 1.99 (t, 2H, *J* = 11.6 Hz), 1.77 (br d, 2H, *J* = 12.7 Hz), 1.75–1.80 (m, 1H), 1.33–1.45 (m, 2H); EIMS *m/e* (rel intensity) 321 (M<sup>+</sup>, 2), 91 (100); EIHRMS calcd for C<sub>20</sub>H<sub>23</sub>N<sub>3</sub>O 321.1842, found 321.1825.

**3-[[2-[1-(Phenylmethyl)-4-piperidinyl]ethyl]amino]-1,2-benzisoxazole (11).** The procedure described for the preparation of **10** was followed with 3-chloro-1,2-benzisoxazole<sup>22</sup> (0.682 g, 4.44 mmol), 4-(aminoethyl)-1-(phenylmethyl)-piperidine (**19**)<sup>13c</sup> (0.970 g, 4.44 mmol), and K<sub>2</sub>CO<sub>3</sub> (0.614 g, 4.44 mmol) in DMSO (30 mL) to give **11** (0.231 g, 15%) as a pale yellow oil: <sup>1</sup>H-NMR (CDCl<sub>3</sub>) δ 7.45–7.54 (m, 2H), 7.24–7.40 (m, 6H), 7.19 (t, 1H, *J* = 7.8 Hz), 4.40 (br t, 1H, *J* = 5.5 Hz), 3.52 (s, 2H), 3.45 (dt, 2H, *J* = 7.4 Hz, *J* = 6.0 Hz), 2.91 (br d, 2H, *J* = 11.8 Hz), 1.99 (br t, 2H, *J* = 11.2 Hz), 1.62–1.73 (m, 4H), 1.37–1.52 (m, 3H); EIMS *m/e* (rel intensity) 335 (M<sup>+</sup>, 10), 91 (100); HRMS calcd for C<sub>21</sub>H<sub>25</sub>N<sub>3</sub>O 335.1999, found 335.1909.

**4-[2-(1,2-Benzisothiazol-3-yl)ethyl]-1-piperidinecarboxylic Acid, 1-(1,1-Dimethylethyl) Ester (25).** Method A was followed with 3-methyl-1,2-benzisothiazole (**24**)<sup>24</sup> (0.50 g, 3.35 mmol), iodide **5** (1.20 g, 3.69 mmol), and 1 M LDA (3.35 mL, 3.35 mmol) in THF (100 mL) to yield **25** (0.582 g, 50%) as a pale yellow oil: <sup>1</sup>H-NMR (CDCl<sub>3</sub>) δ 7.91–7.96 (m, 2H), 7.43–7.52 (m, 2H), 4.05–4.14 (m, 2H), 3.15 (t, 2H, *J* = 7.9 Hz), 2.69 (br t, 2H, *J* = 12.1 Hz), 1.74–1.88 (m, 4H), 1.46–1.60 (m, 1H), 1.46 (s, 9H), 1.10–1.29 (m, 2H); EIMS *m/e* (rel intensity) 346 (M<sup>+</sup>, 60), 57 (100); EIHRMS calcd for C<sub>19</sub>H<sub>26</sub>N<sub>2</sub>O<sub>2</sub>S 346.1716, found 346.1724.

**3-[2-[1-(Phenylmethyl)-4-piperidinyl]ethyl]-1,2-benzisothiazole, Maleate Salt (20).** Method C was followed with **25** (0.312 g, 0.90 mmol) and trifluoroacetic acid (2.3 mL) in CH<sub>2</sub>Cl<sub>2</sub> (10 mL) followed by triethylamine (0.837 mL, 6.0 mmol) and benzyl bromide (0.154 mL, 1.30 mmol) in CH<sub>2</sub>Cl<sub>2</sub> (10 mL) to give **20**, free base (0.223 g, 74%) as a clear oil. The maleate salt was prepared by adding a solution of maleic acid (0.077 g, 0.66 mmol) dissolved in the minimum amount of EtOH to a solution of the free base (0.223 g, 0.66 mmol) in CH<sub>2</sub>Cl<sub>2</sub> (12 mL). The resulting mixture was concentrated, and the residue was purified by recrystallization from EtOAc to give **20**, maleate salt (0.210 g, 70%): mp (EtOAc) 175–176 °C; <sup>1</sup>H-NMR (CDCl<sub>3</sub>) δ 8.14–8.21 (m, 2H), 7.63 (t, 1H, *J* = 7.4 Hz), 7.50–7.55 (m, 6H), 6.04 (s, 2H), 4.26 (br s, 2H), 3.35 (br s, 2H), 3.15 (t, 2H, *J* = 7.6 Hz), 2.80–2.92 (m, 2H), 1.92–2.00 (m, 2H), 1.78–1.88 (m, 2H), 1.54–1.65 (m, 1H), 1.35–1.45 (m, 2H); EIMS *m/e* (rel intensity) 336 (M<sup>+</sup>, 10), 91 (100). Anal. (C<sub>21</sub>H<sub>24</sub>N<sub>2</sub>S·C<sub>4</sub>H<sub>4</sub>O<sub>4</sub>) C, H, N.

**4-[2-(Isoquinol-1-yl)ethyl]-1-piperidinecarboxylic Acid, 1-(1,1-Dimethylethyl) Ester (27).** Method A was followed with 1-methylisoquinoline (**26**) (0.50 g, 3.49 mmol), iodide **5** (1.2 g, 3.84 mmol), and 1 M LDA (4.2 mL, 4.2 mmol) in THF (45 mL) at –78 °C for 1.75 h. Purification by silica gel flash chromatography (30% EtOAc-toluene) gave **27** (0.784 g, 66%) as a yellow oil: <sup>1</sup>H-NMR (CDCl<sub>3</sub>) δ 8.38 (d, 1H, *J* = 5.8 Hz), 8.08 (d, 1H, *J* = 8.3 Hz), 7.77 (d, 1H, *J* = 8.0 Hz), 7.62 (t, 1H, *J* = 7.1 Hz), 7.54 (t, 1H, *J* = 7.1 Hz), 7.46 (d, 1H, *J* = 5.7 Hz), 4.08 (br s, 2H), 3.25–3.30 (m, 2H), 2.67 (br t, 2H, *J* = 12.3 Hz), 1.73–1.81 (m, 4H), 1.49–1.63 (m, 1H), 1.42 (s, 9H), 1.17 (ddd, 2H, *J* = 24.6 Hz, *J* = 12.1 Hz, *J* = 3.8 Hz); EIMS *m/e* (rel intensity) 340 (M<sup>+</sup>, 10), 156 (100); EIHRMS calcd for C<sub>21</sub>H<sub>28</sub>N<sub>2</sub>O<sub>2</sub> 340.2151, found 340.2130.

**1-[2-[1-(Phenylmethyl)-4-piperidinyl]ethyl]isoquinoline, Maleate Salt (21).** Method C was followed with **27** (0.713 g, 2.10 mmol) and trifluoroacetic acid (7 mL) in CH<sub>2</sub>Cl<sub>2</sub> (14 mL) followed by triethylamine (2.9 mL, 21.0 mmol) and benzyl bromide (0.275 mL, 2.31 mmol) in CH<sub>2</sub>Cl<sub>2</sub> (60 mL) to give **21**, free base (0.26 g, 38%) as a pale yellow oil. The monomaleate salt was prepared by adding a solution of maleic

acid (0.10 g, 0.867 mmol) in EtOH (3 mL) to a solution of the free base (0.26 g, 0.788 mmol) in CH<sub>2</sub>Cl<sub>2</sub> (7 mL). After concentrating, the salt was purified by recrystallization [cold (0 °C) EtOAc] to give **21**, maleate salt (0.195 g, 56%) as an off-white solid: mp 136–137 °C dec; <sup>1</sup>H-NMR (DMSO-*d*<sub>6</sub>) δ 8.39 (d, 1H, *J* = 5.7 Hz), 8.26 (d, 1H, *J* = 8.3 Hz), 7.97 (d, 1H, *J* = 8.1 Hz), 7.77 (t, 1H, *J* = 7.4 Hz), 7.66–7.71 (m, 2H), 7.49 (s, 5H), 6.05 (s, 2H), 4.28 (br s, 2H), 3.27–3.32 (m, 2H), 2.87–2.90 (m, 2H), 1.76–2.03 (m, 6H), 1.55–1.69 (m, 1H), 1.33–1.46 (m, 2H); EIMS *m/e* (rel intensity) 330 (M<sup>+</sup>, 50), 239 (100). Anal. (C<sub>23</sub>H<sub>26</sub>N<sub>2</sub>·C<sub>4</sub>H<sub>4</sub>O<sub>4</sub>·0.5H<sub>2</sub>O) C, H, N.

**4-[2-(1,3-Quinazol-4-yl)ethyl]-1-piperidinecarboxylic Acid, 1-(1,1-Dimethylethyl) Ester (28).** Freshly prepared 1 M LDA (4.2 mL, 4.2 mmol) was added to a solution of 4-methyl-1,3-quinazoline (0.60 g, 4.2 mmol) in THF (35 mL) at 0 °C. To the yellow solution obtained was added neat trimethylsilyl chloride (0.53 mL, 4.2 mmol). After 3 min, a second equivalent of 1 M LDA (4.2 mL, 4.2 mmol) was added. Next, a solution of iodide **5** (1.49 g, 4.6 mmol) in THF (10 mL) was added, and stirring was continued at 0 °C for 1 h. HCl (1 N) was added, and the mixture was stirred at room temperature for 30 min. The reaction mixture was made basic by addition of 1 N NaOH and extracted with EtOAc. The organic layer was washed with brine, dried (MgSO<sub>4</sub>), filtered, and concentrated. Purification by silica gel flash chromatography (20% – 50% EtOAc-hexanes) gave **28** (0.466 g, 33%) as an oil: <sup>1</sup>H-NMR (CDCl<sub>3</sub>) δ 9.21 (s, 1H), 8.12 (d, 1H, *J* = 7.7 Hz), 8.05 (d, 1H, *J* = 8.4 Hz), 7.90 (t, 1H, *J* = 7.8 Hz), 7.65 (t, 1H, *J* = 7.7 Hz), 4.08–4.17 (m, 2H), 3.32 (t, 2H, *J* = 8.3 Hz), 2.72 (br t, 2H, *J* = 12.1 Hz), 1.78–1.90 (m, 4H), 1.57–1.59 (m, 1H), 1.47 (s, 9H), 1.18–1.29 (m, 2H); EIMS *m/e* (rel intensity) 341 (M<sup>+</sup>, 10), 157 (100); EIHRMS calcd for C<sub>20</sub>H<sub>27</sub>N<sub>3</sub>O<sub>2</sub> 341.2104, found 341.2099.

**4-[2-[1-(Phenylmethyl)-4-piperidinyl]ethyl]-1,3-quinazoline, Maleate Salt (22).** Method C was followed with **28** (0.429 g, 1.26 mmol) and trifluoroacetic acid (3.5 mL) in CH<sub>2</sub>Cl<sub>2</sub> (13 mL) followed by triethylamine (0.88 mL, 6.3 mmol) and benzyl bromide (0.17 mL, 1.39 mmol) in CH<sub>2</sub>Cl<sub>2</sub> (22 mL) to give **22**, free base (0.179 g, 43%) as a colorless oil. The maleate salt was prepared by adding a solution of maleic acid (0.052 g, 0.45 mmol) in Et<sub>2</sub>O (10 mL) to a solution of the free base (0.135 g, 0.41 mmol) in Et<sub>2</sub>O (200 mL). The white solid obtained was collected by filtration to give **22**, maleate salt (0.103 g, 56%): mp 121–122 °C; <sup>1</sup>H-NMR (DMSO-*d*<sub>6</sub>) δ 9.16 (s, 1H), 8.33 (d, 1H, *J* = 8.4 Hz), 7.98–8.01 (m, 2H), 7.72–7.78 (m, 1H), 7.43 (s, 5H), 6.02 (s, 2H), 4.08 (br s, 2H), 3.32 (t, 2H, *J* = 7.7 Hz), 3.15–3.35 (m, 2H), 2.60–2.80 (m, 2H), 1.89–1.94 (m, 2H), 1.76–1.79 (m, 2H), 1.30–1.60 (m, 3H); EIMS *m/e* (rel intensity) 331 (M<sup>+</sup>, 10), 77 (100). Anal. (C<sub>22</sub>H<sub>28</sub>N<sub>3</sub>·C<sub>4</sub>H<sub>4</sub>O<sub>4</sub>) C, H, N.

**1-(2-Fluorophenyl)-3-[1-(phenylmethyl)-4-piperidinyl]propanone (29).** Lithium hexamethyldisilazide (1 M, 14.5 mL, 14.5 mmol) was added to a solution of *o*-fluoroacetophenone (2.0 g, 14.5 mmol) in THF (100 mL) at –78 °C. The mixture obtained was allowed to warm to –20 °C over a 30–60 min period and then recooled to –78 °C. A solution of aldehyde **16**<sup>54</sup> (2.94 g, 14.5 mmol) in THF (20 mL) was added. The mixture was kept at –78 °C for 30 min and then allowed to warm to room temperature and stirred for 40 min. Saturated NH<sub>4</sub>Cl was added, and the reaction mixture was extracted with EtOAc. The organic layer was dried (MgSO<sub>4</sub>), filtered, and concentrated. Purification by silica gel flash chromatography (30% – 50% EtOAc-CH<sub>2</sub>Cl<sub>2</sub>) gave a yellow oil (2.14 g). <sup>1</sup>H-NMR showed a mixture of compounds (two major components). Further purification was not attempted.

A portion of the mixture obtained above (0.661 g) and PtO<sub>2</sub> (0.070 g, 0.31 mmol) in EtOH was hydrogenated in a Parr shaker at 48 psi for 2 h. The mixture was filtered through a Celite pad, and the filtrate was concentrated. An additional reaction with the above mixture (1.00 g) was also carried out. Crude products from these reactions were combined and purified by silica gel flash chromatography (1% – 3% MeOH-CH<sub>2</sub>Cl<sub>2</sub>) to give **29** (0.192 g, 5.3% overall) as a colorless oil: <sup>1</sup>H-NMR (CDCl<sub>3</sub>) δ 7.85 (dt, 1H, *J* = 7.6 Hz, *J* = 1.8 Hz), 7.47–7.56 (m, 1H), 7.09–7.33 (m, 7H), 3.49 (s, 2H), 2.95–3.03 (m, 2H), 2.89 (br d, 2H, *J* = 11.4 Hz), 1.94 (br t, 2H, *J* = 11.1 Hz),

1.63–1.77 (m, 4H), 1.24–1.39 (m, 3H); EIMS  $m/e$  (rel intensity) 325 ( $M^+$ , 15), 91 (100); EIHRMS calcd for  $C_{21}H_{24}FNO$  325.1842, found 325.1866.

**3-[2-[1-(Phenylmethyl)-4-piperidinyl]ethyl]-1H-indazole Maleate Salt (23).** A mixture of **29** (0.178 g, 0.55 mmol) in anhydrous hydrazine (10 mL) was heated to reflux for 3 h. The reaction mixture was allowed to cool,  $H_2O$  was added, and the mixture was extracted with  $CH_2Cl_2$ . The organic layer was dried ( $MgSO_4$ ), filtered, and concentrated. Purification by silica gel radial chromatography ( $CH_2Cl_2$ –10% MeOH- $CH_2Cl_2$ ) gave **23**, free base (0.047 g, 27%) as a colorless oil. The maleate salt was prepared by adding a solution of maleic acid (0.010 g, 0.085 mmol) in  $Et_2O$  (5 mL) to a solution of the free base (0.027 g, 0.085 mmol) in  $Et_2O$  (75 mL). The white solid obtained was collected by filtration to give **23**, maleate salt (0.014 g, 38%): mp 152–153 °C;  $^1H$ -NMR ( $DMSO-d_6$ )  $\delta$  12.7 (s, 1H), 7.72 (d, 1H,  $J = 8.0$  Hz), 7.44–7.47 (m, 6H), 7.31 (t, 1H,  $J = 7.3$  Hz), 7.06 (t, 1H,  $J = 7.4$  Hz), 6.02 (s, 2H), 4.24 (br s, 2H), 2.93 (t, 2H,  $J = 7.6$  Hz), 1.90–2.00 (m, 2H), 1.60–1.80 (m, 3H), 1.30–1.50 (m, 4H); EIMS  $m/e$  (rel intensity) 319 ( $M^+$ , 25), 91 (100); EIHRMS calcd for  $C_{21}H_{25}N_3$  319.2049, found 319.2029.

**Inhibition of Acetylcholinesterase and Butyrylcholinesterase.** The method of Ellman *et al.*<sup>26</sup> was followed. The assay solution consisted of a 0.1 M sodium phosphate buffer, pH 8.0, with the addition of 100  $\mu M$  tetraisopropylpyrophosphoramide (*iso*-OMPA), 100  $\mu M$  5,5'-dithiobis(2-nitrobenzoic acid) (DTNB), 0.02 unit/mL AChE (Sigma Chemical Co.; from human erythrocytes), and 200  $\mu M$  acetylthiocholine iodide. The final assay volume was 0.25 mL. Test compounds were added to the assay solution prior to enzyme addition, whereupon a 20 min preincubation period with enzyme was followed by addition of substrate. Changes in absorbance at 412 nm were recorded for 5 min. The reaction rates were compared, and the percent inhibition due to the presence of test compounds was calculated.

Inhibition of butyrylcholinesterase was measured as described above for AChE by omitting addition of *iso*-OMPA and substituting 0.02 unit/mL BuChE (Sigma Chemical Co.; from horse serum) and 200  $\mu M$  butyrylthiocholine for enzyme and substrate, respectively.

**Measurement of Elevation of Acetylcholine in Mouse Brain.** AChE inhibitors were given orally. Animals were sacrificed by focused microwave irradiation at 1 h postdosing, and the forebrains were removed and homogenized in 20 mM sodium phosphate buffer, pH 5.3. Homogenates were centrifuged 20 min at 12000g; supernatants (10–20  $\mu L$ ) were used for determination of ACh with an ACh analysis system from Bioanalytical Systems (West Lafayette, IN). A polymeric anion-exchange column resolved ACh from choline (Ch), and a postcolumn reactor column containing immobilized AChE and Ch oxidase converted ACh and Ch to betaine and hydrogen peroxide; the hydrogen peroxide was readily measured with an electrochemical detector at 500 mV vs Ag/AgCl reference electrode and a platinum working electrode. Sensitivity was approximately 3–5 pmol of ACh. Typical ACh control values were 18–25 nmol/g in mouse forebrain. Data for drug-treated animals are reported as percent control values. In general, the treatment consisted of eight animals per group. Statistical significance was determined by Student's one-tailed *t*-test.

**Passive Avoidance.** A one-trial step-through passive avoidance procedure was used which is similar to that utilized by Bammer.<sup>55</sup> At the training session, animals were treated with drugs, placed in the lighted side of a shuttle chamber, and allowed to cross over to the nonlighted side, where a scrambled, constant current footshock was delivered until the mouse escaped to the original, lighted side. Following a 24 h delay with no additional drug treatment, animals were tested by placing them in the lighted side and determining step-through latency.

Training step-through latency was typically 25–35 s, with a typical escape crossover time of 3–4 s. For vehicle treated animals (controls), step-through latency at the retention test session was typically 150–210 s, indicative of memory of the training session footshock. A statistically significant decrease in the test session step-through latency was interpreted as

evidence for amnesia. In the training session, animals which did not cross over to the dark side within 90 s were discarded, as were animals which did not escape the footshock within 20 s. In the test session, animals which did not cross over within 300 s were assigned a step-through latency of 300 s.

**Acknowledgment.** The authors wish to thank Mr. P. Reiche, Mr. M. S. Teague, Mr. R. S. Ware, and Mr. S. C. Maginess for mass spectra and NMR support. We are also grateful to Dr. Julian Tirado-Rives (Yale University) for providing us with various molecular dynamics analysis programs.

**Supplementary Material Available:** OPLS parameters for inhibitor **1g** (2 pages). Ordering information is given on any current masthead page.

## References

- (1) (a) Perry, E. K. The Cholinergic Hypothesis - Ten Years On. *Br. Med. Bull.* **1986**, *42*, 63–69. (b) Bartus, R. T.; Dean, L. D., III; Beer, B.; Lippa, A. S. The Cholinergic Hypothesis of Geriatric Memory Dysfunction. *Science* **1982**, *217*, 408–417.
- (2) (a) Sims, N. R.; Bowen, D. M.; Allen, S. J.; Smith, C. C. T.; Neary, D.; Thomas, D. J.; Davison, A. N. Presynaptic Cholinergic Dysfunction in Patients with Dementia. *J. Neurochem.* **1983**, *40*, 503–509. (b) Rossor, M. N.; Reffeld, J. F.; Emson, P. C.; Mountjoy, C. Q.; Roth, M.; Iversen, L. L. Normal Cortical Concentration of Cholecystinin-like Immunoreactivity with Reduced Choline Acetyltransferase Activity in Senile Dementia of Alzheimer's Type. *Life Sci.* **1981**, *29*, 405–410.
- (3) (a) Vogels, O. J. M.; Broere, C. A. J.; Ter Laak, H. J.; Ten Donkelaar, H. J.; Nieuwenhuys, R.; Schulte, B. P. M. Cell Loss and Shrinkage in the Nucleus Basalis Meynert Complex in Alzheimer's Disease. *Neurobiol. Aging* **1990**, *11*, 3–13. (b) Whitehouse, P. J.; Price, D. L.; Struble, R. G.; Clark, A. W.; Coyle, J. T.; DeLong, M. R. Alzheimer's Disease and Senile Dementia: Loss of Neurons in the Basal Forebrain. *Science* **1982**, *215*, 1237–1239.
- (4) (a) Sitaram, N.; Weingartner, H.; Gillin, J. C. Human Serial Learning: Enhancement with Arecoline and Choline and Impairment with Scopolamine. *Science* **1978**, *201*, 274–276. (b) Drachman, D. A. Memory and Cognitive Function in Man: Does the Cholinergic System have a Specific Role? *Neurology* **1977**, *27*, 783–790.
- (5) (a) John, V.; Lieberburg, I.; Thorsett, E. D. Alzheimer's Disease: Current Therapeutic Approaches. *Annu. Rep. Med. Chem.* **1993**, *28*, 197–206. (b) Davidson, M.; Stern, R. G.; Bierer, L. M.; Horvath, T. B.; Zemishlani, Z.; Markofsky, R.; Mohs, R. C. Cholinergic Strategies in the Treatment of Alzheimer's Disease. *Acta Psychiatr. Scand., Suppl.* **1991**, *366*, 47–51. (c) Moos, W. H.; Hershenson, F. M. Potential Therapeutic Strategies for Senile Cognitive Disorders. *DN&P* **1989**, *2*, 397–409.
- (6) (a) Kumar, V.; Calache, M. Treatment of Alzheimer's Disease with Cholinergic Drugs. *Int. J. Clin. Pharmacol., Ther. Toxicol.* **1991**, *29*, 23–37. (b) Becker, R. E.; Giacobini, E. Mechanisms of Cholinesterase Inhibition in Senile Dementia of the Alzheimer's Type: Clinical, Pharmacological, and Therapeutic Aspects. *Drug Dev. Res.* **1988**, *12*, 163–195.
- (7) (a) Knapp, M. J.; Knopman, D. S.; Solomon, P. R.; Pendlebury, W. W.; Davis, C. S.; Gracon, S. I. A 30-Week Randomized Controlled Trial of High-Dose Tacrine in Patients with Alzheimer's Disease. *J. Am. Med. Assoc.* **1994**, *271*, 985–998. (b) Farlow, M.; Gracon, S. I.; Hershey, L. A.; Lewis, K. W.; Sadowsky, C. H.; Dolan-Ureno, J. A Controlled Trial of Tacrine in Alzheimer's Disease. *J. Am. Med. Assoc.* **1992**, *268*, 2523–2529.
- (8) *Scrip* **1993**, 1856, 19.
- (9) Summers, W. K.; Koehler, A. L.; Marsh, G. M.; Tachiki, K.; Kling, A. Long-term Hepatotoxicity of Tacrine. *Lancet* **1989**, *1*, 729. (b) Marx, J. L. Alzheimer's Drug Trial Put on Hold. *Science* **1987**, *238*, 1041–1042.
- (10) Woolf, T. F.; Pool, W. F.; Bjorge, S. M.; Chang, T.; Goel, O. P.; Purchase, C. F., II; Schroeder, M. C.; Kunze, K. L.; Trager, W. F. Bioactivation and Irreversible Binding of the Cognition Activator Tacrine Using Human and Rat Liver Microsomal Preparations. *Drug Metab. Dispos.* **1993**, *21*, 874–882.
- (11) Giacobini, E.; Somani, S.; McIlhany, M.; Downen, M.; Hallak, M. Pharmacokinetics and Pharmacodynamics of Physostigmine after I. V. Administration in Beagle Dogs. *Neuropharmacology* **1987**, *26*, 831–836.
- (12) *Scrip* **1992**, 1775, 25.
- (13) (a) Sugimoto, H.; Iimura, Y.; Yamanishi, Y.; Yamatsu, K. Synthesis and Anti-Acetylcholinesterase Activity of 1-Benzyl-4-[(5,6-dimethoxy-1-indanon-2-yl)methyl]piperidine hydrochloride (E2020) and Related Compounds. *Bioorg. Med. Chem. Lett.* **1992**, *2*, 871–876. (b) Sugimoto, H.; Tsuchiya, Y.; Sugumi, H.;

- Higurashi, K.; Karibe, N.; Iimura, Y.; Sasaki, A.; Araki, S.; Yamanishi, Y.; Yamatsu, K. Synthesis and Structure-Activity Relationships of Acetylcholinesterase Inhibitors: 1-Benzyl-4-(2-phthalimidoethyl)piperidine and Related Derivatives. *J. Med. Chem.* **1992**, *35*, 4242-4548. (c) Sugimoto, H.; Tsuchiya, Y.; Sugumi, H.; Higurashi, K.; Karibe, N.; Iimura, Y.; Sasaki, A.; Kawakami, Y.; Nakamura, T.; Araki, S.; Yamanishi, Y.; Yamatsu, K. Novel Piperidine Derivatives. Synthesis and Anti-Acetylcholinesterase Activity of 1-Benzyl-4-[2-(N-benzoylamino)ethyl]piperidine Derivatives. *J. Med. Chem.* **1990**, *33*, 1880-1887.
- (14) Mihara, M.; Ohnishi, A.; Tomono, Y.; Hasegawa, J.; Shimamura, Y.; Yamazaki, K.; Morishita, N. Pharmacokinetics of E2020, a New Compound for Alzheimer's Disease, in Healthy Male Volunteers. *Int. J. Clin. Pharmacol., Ther. Toxicol.* **1993**, *31*, 223-229.
- (15) For use of the benzisoxazole and isoxazole heterocycles as carbonyl bioisosteres, see: (a) Mewshaw, R. E.; Silverman, L. S.; Mathew, R. M.; Kaiser, C.; Sherrill, R. G.; Cheng, M.; Tiffany, C. W.; Karbon, E. W.; Bailey, M. A.; Borosky, S. A.; Ferkany, J. W.; Abreu, M. E. Bridged  $\gamma$ -Carbolines and Derivatives Possessing Selective and Combined Affinity for 5-HT<sub>2</sub> and D<sub>2</sub> Receptors. *J. Med. Chem.* **1993**, *36*, 1488-1495. (b) Strupczewski, J. T.; Allen, R. C.; Gardner, B. A.; Schmid, B. L.; Stache, U.; Glamkowski, E. J.; Jones, M. C.; Ellis, D. B.; Huger, F. P.; Dunn, R. W. Synthesis and Neuroleptic Activity of 3-(1-Substituted-4-piperidinyl)-1,2-benzisoxazoles. *J. Med. Chem.* **1985**, *28*, 761-769. (c) Krogsgaard-Larsen, P.; Jensen, B.; Falch, E.; Jorgensen, F. S. Heterocyclic Muscarinic Agonists: Structural and Therapeutic Aspects. *Drugs Fut.* **1989**, *14*, 541-561.
- (16) Thakar, K. A.; Goswami, D. D.; Bhawal, B. M. A Modified Method for the Synthesis of 1,2-Benzisoxazoles. *Indian J. Chem.* **1977**, *15B*, 1058-1059.
- (17) Chen, F. C.; Chang, C. T. Synthesis of 7-Halogenoflavone and Related Compounds. *J. Chem. Soc.* **1958**, 146-150.
- (18) Verboom, W.; Reinhoudt, D. N.; Visser, R.; Harkema, S. "tert-Amino Effect" in Heterocyclic Synthesis. Formation of N-Heterocycles by Ring-Closure Reactions of Substituted 2-Vinyl-N,N-dialkylanilines. *J. Org. Chem.* **1984**, *49*, 269-276.
- (19) Oliver, J. E.; Waters, R. M.; Lusby, W. R. Alkylation and Rearrangement of Lithiated 3-Methyl-1,2-benzisoxazoles. *J. Org. Chem.* **1989**, *54*, 4970-4973.
- (20) Hall, J. H.; Gislser, M. A Simple Method for Converting Nitriles to Amides. Hydrolysis with Potassium Hydroxide in *tert*-Butyl Alcohol. *J. Org. Chem.* **1976**, *41*, 3769-3770.
- (21) Naruto, S.; Mizuta, H.; Yoshida, T.; Uno, H.; Kawashima, K.; Kadokawa, T.; Nishimura, H. Synthesis and Spasmolytic Activity of 2-Substituted-3-( $\omega$ -dialkylamino-alkoxyphenyl)acrylonitriles and Related Compounds. *Chem. Pharm. Bull.* **1983**, *31*, 2023-2032.
- (22) Boshagen, H. Über 3-Chlor-1,2-benzisoxazole. (3-Chloro-1,2-benzisoxazoles.) *Chem. Ber.* **1967**, *100*, 3326-3330.
- (23) Pascal, G.; Sevrin, M.; Mangane, M. [(4-Piperidyl)methyl]-2,3-dihydro-1H-isoindole and 2,3,4,5-Tetrahydro-1H-benzazepine Derivatives, Their Preparation and Their Application in Therapy. US Patent 5,096,900, March 17, 1992.
- (24) McKinnon, D. M.; Lee, K. R. Fused Heterocycles from *o*-Acylbenzenethiol Derivatives. *Can. J. Chem.* **1988**, *66*, 1405-1409.
- (25) Behr, L. C.; Fusco, R.; Jarboe, C. H. Pyrazoles, Pyrazolines, Pyrazolidines, Indazoles and Condensed Rings. In *The Chemistry of Heterocyclic Compounds*; Wiley, R. H., Ed; Interscience Publishers: New York, 1967; Vol. 22, pp 289-366.
- (26) Ellman, G. L.; Courtney, K. D.; Andres, V., Jr.; Featherstone, R. M. A New and Rapid Colorimetric Determination of Acetylcholinesterase Activity. *Biochem. Pharmacol.* **1961**, *7*, 88-95.
- (27) Thomsen, T.; Zende, B.; Fischer, J. P.; Kewitz, H. *In Vitro* Effects of Various Cholinesterase Inhibitors on Acetyl- and Butyrylcholinesterase of Healthy Volunteers. *Biochem. Pharmacol.* **1991**, *41*, 139-141 and references cited therein.
- (28) Sussman, J. L.; Harel, M.; Frolow, F.; Oefner, C.; Goldman, A.; Tokar, L.; Silman, I. Atomic Structure of Acetylcholinesterase from *Torpedo californica*: A Prototypic Acetylcholine-Binding Protein. *Science* **1991**, *253*, 872-879.
- (29) Jorgensen, W. L.; Severance, D. L. Aromatic-Aromatic Interactions: Free Energy Profiles for the Benzene Dimer in Water, Chloroform, and Liquid Benzene. *J. Am. Chem. Soc.* **1990**, *112*, 4768-4774.
- (30) Harel, M.; Schalk, I.; Ehret-Sabatier, L.; Bouet, F.; Goeldner, M.; Hirth, C.; Axelsen, P.; Silman, I.; Sussman, J. L. Quaternary Ligand Binding to Aromatic Residues in the Active-Site Gorge of Acetylcholinesterase. *Proc. Natl. Acad. Sci. U.S.A.* **1993**, *90*, 9031-9035.
- (31) Soreq, H. E.; Ben-Aziz, R.; Prody, C. A.; Seidman, S.; Gnatt, A.; Neville, L.; Lieman-Hurwitz, J.; Lev-Lehman, E.; Ginzberg, D.; Lapidot-Lifson, Y.; Zakut, H. Molecular Cloning and Construction of the Coding Region for Human Acetylcholinesterase Reveals a G+C-Rich Attenuating Structure. *Proc. Natl. Acad. Sci. U.S.A.* **1990**, *87*, 9688-9692.
- (32) Pearlman, D. A.; Case, D. A.; Caldwell, J. C.; Seibel, G. L.; Singh, U. C.; Weiner, P.; Kollman, P. A. AMBER 4.0, University of California: San Francisco, 1990.
- (33) Jorgensen, W. L.; Tirado-Rives, J. The OPLS Potential Functions for Proteins. Energy Minimization for Crystals of Cyclic Peptides and Crambin. *J. Am. Chem. Soc.* **1988**, *110*, 1657-1666.
- (34) Jorgensen, W. L.; Chandrasekhar, J.; Madura, J. D.; Impey, R. W.; Klein, M. L. Comparison of Simple Potential Functions for Simulating Liquid Water. *J. Chem. Phys.* **1983**, *79*, 926-935.
- (35) Jorgensen, W. L. Free Energy Calculations: A Breakthrough for Modeling Organic Chemistry in Solution. *Acc. Chem. Res.* **1989**, *22*, 184-189.
- (36) Jorgensen, W. L.; Nguyen, T. B. Monte Carlo Simulations of the Hydration of Substituted Benzenes with OPLS Potential Functions. *J. Comput. Chem.* **1993**, *14*, 195-205.
- (37) Jorgensen, W. L.; Laird, E. R.; Nguyen, T. B.; Tirado-Rives, J. Monte Carlo Simulations of Pure Liquid Substituted Benzenes with OPLS Potential Functions. *J. Comput. Chem.* **1993**, *14*, 206-215.
- (38) Jorgensen, W. L.; Gao, J. Monte Carlo Simulations of the Hydration of Ammonium and Carboxylate Ions. *J. Phys. Chem.* **1986**, *90*, 2174-2182.
- (39) Jorgensen, W. L.; Madura, J. D.; Swenson, C. J. Optimized Intermolecular Potential Functions for Liquid Hydrocarbons. *J. Am. Chem. Soc.* **1984**, *106*, 6638-6646.
- (40) Breneman, C. M.; Wiberg, K. B. Determining Atom-Centered Monopoles from Molecular Electrostatic Potentials. The Need for High Sampling Density in Formamide Conformational Analysis. *J. Comput. Chem.* **1990**, *3*, 361-373.
- (41) (a) Francl, M. M.; Pietro, W. J.; Hehre, W. J.; Binkley, J. S.; Gordon, M. S.; DeFrees, D. J.; Pople, J. A. Self-Consistent Molecular Orbital Methods. XXIII. A Polarization-Type Basis Set for Second-Row Elements. *J. Chem. Phys.* **1982**, *77*, 3654-3665. (b) Binkley, J. S.; Pople, J. A.; Hehre, W. J. Self-Consistent Molecular Orbital Methods. 21. Small Split-Valence Basis Sets for First-Row Elements. *J. Am. Chem. Soc.* **1980**, *102*, 939-947.
- (42) Schlegel, H. B. Optimization of Equilibrium Geometries and Transition Structures. *J. Comput. Chem.* **1982**, *3*, 214-218.
- (43) Frisch, M. J.; Trucks, G. W.; Head-Gordon, M.; Gill, P. M. W.; Wong, M. W.; Foresman, J. B.; Johnson, B. G.; Schlegel, H. B.; Robb, M.; Replogle, E. S.; Gomperts, R.; Andres, J. L.; Raghavachari, K.; Binkley, J. S.; Gonzalez, C.; Martin, R. L.; Fox, D. J.; DeFrees, D. J.; Baker, J.; Stewart, J. J. P.; Pople, J. A. *Gaussian92 Version C*; Gaussian, Inc.: Pittsburgh, PA, 1992.
- (44) Carlson, H. A.; Nguyen, T. B.; Orozco, M.; Jorgensen, W. L. Accuracy of Free Energies of Hydration for Organic Molecules from 6-31G\*-Derived Partial Charges. *J. Comput. Chem.* **1993**, *14*, 1240-1249.
- (45) (a) Weiner, S. J.; Kollman, P. A.; Case, D. A.; Singh, U. C.; Ghio, C.; Alagona, G.; Profeta, S., Jr.; Weiner, P. A New Force Field for Molecular Mechanical Simulation of Nucleic Acids and Proteins. *J. Am. Chem. Soc.* **1984**, *106*, 765-784. (b) Pranata, J.; Jorgensen, W. L. Computational Studies on FK506: Conformational Search and Molecular Dynamics Simulation in Water. *J. Am. Chem. Soc.* **1991**, *113*, 9483-9493.
- (46) Ryckaert, J.-P.; Cicotti, G.; Berendsen, H. J. C. Numerical Integration of the Cartesian Equations of Motion of a System with Constraints: Molecular Dynamics of *n*-Alkanes. *J. Comput. Phys.* **1977**, *23*, 327-341.
- (47) Bernstein, F. C.; Koetzle, T. F.; Williams, G. J. B.; Meyer, E. F., Jr.; Brice, M. D.; Rodgers, J. R.; Kennard, O.; Shimanouchi, T. M.; Tasumi, M. The Protein Data Bank: A Computer-based Archival File for Macromolecular Structures. *J. Mol. Biol.* **1977**, *112*, 535-542.
- (48) SYBYL Version 6.03; Tripos Associates, Inc., 1699 S. Hanley Rd., Suite 303, St. Louis, MO 63144.
- (49) Pang, Y.-P.; Kozikowski, A. Prediction of the Binding Site of 1-Benzyl-4-[(5,6-dimethoxy-1-indanon-2-yl)methyl]piperidine in Acetylcholinesterase by Docking Studies with the SYSDOC Program. Submitted for publication.
- (50) Lindemann, H.; Konitzer, H.; Romanoff, S. Zur Kenntnis der Indoxazene. (Indoxazenes.) *Liebigs Ann. Chem.* **1929**, *456*, 284-311.
- (51) Sahasrabudhe, A. B.; Kamath, S. V.; Bapat, B. V.; Bhawal, B. M.; Kulkarni, S. N. Antitubercular Agents: Part VI - Alkoxy Derivatives of 6-Hydroxy-3-methyl-1,2-benzisoxazole. *Indian J. Chem.* **1983**, *22B*, 1266-1267.
- (52) Borsche, W.; Hahn-Weinheimer, P. Zur Kenntnis der Benzisoxazole. VI. Die Acylierung von Benzisoxazolen nach Friedel-Crafts. (Benzisoxazoles. VI. Friedel-Crafts Acylation of Benzisoxazoles.) *Liebigs Ann. Chem.* **1950**, *570*, 155-164.
- (53) Efang, S. M. N.; Michelson, R. H.; Knusel, B.; Hefti, F.; Boudreau, R. J.; Thomas, J. R.; Tennison, J. R. Synthesis and Biological Evaluation of Radioiodinated N-2-(4-Piperidyl)ethylbenzamide. *Nucl. Med. Biol.* **1993**, *20*, 527-538.
- (54) Hermans, B.; Van Daele, P. Synthesis of 1-Benzyl-4-formylpiperidine. *Ind. Chim. Belge* **1967**, *32*, 64-65.
- (55) Bammer, G. Pharmacological Investigations of Neurotransmitter Involvement in Passive Avoidance Responding: A Review and Some New Results. *Neurosci. Biobehav. Rev.* **1982**, *6*, 247-296.